



Degree Project in Electrical Engineering

Second cycle, 30 credits

Comparison and Evaluation of Generation Shift Key Strategies in Flow-Based Market Coupling

JOHANES HENDRA FEBRIANTO RAJAGUKGUK

Comparison and Evaluation of Generation Shift Key Strategies in Flow-Based Market Coupling

JOHANES HENDRA FEBRIANTO RAJAGUKGUK

Master's Programme, Electric Power Engineering, 120 credits
Date: October 24, 2025

Supervisor: Mohammad Reza Karimi Gharigh
Examiner: Mohammad Reza Hesamzadeh

School of Electrical Engineering and Computer Science

Swedish title: Jämförelse och utvärdering av strategier för generation shift key i
flödesbaserad marknadskoppling

Abstract

This thesis presents a comprehensive analysis and evaluation of generation shift key (GSK) approaches within flow-based market coupling (FBMC) simulation for power systems. As European electricity markets transition toward full liberalization through regional market coupling, FBMC has emerged as a critical methodology for optimizing cross-border electricity trading while accounting for transmission network constraints. However, the strategies and methods for calculating GSKs remain underdetermined and require further investigation.

This study develops a mathematical framework that presents the transmission model in the FBMC, encompassing nodal optimal power flow, FBMC optimization, and redispatch modeling. In this research, five GSK strategies are examined, including two novel approaches. The proposed strategies include one with non-negativity constraints and another that allows negative values for enhanced flexibility. These are compared against existing GSK strategies through comprehensive simulations.

The methodology employs a system with three zones, examining four seasonal cases under both perfect and imperfect forecasting scenarios. Each case incorporates realistic load and renewable energy variations. Results demonstrate that the proposed GSK strategies offer significant adaptability advantages over traditional approaches. The total operational costs analysis reveals that the proposed GSK strategies can achieve cost reductions compared to existing approaches. The methods also show a better performance in system marginal cost optimization and reduced redispatch requirements under forecast uncertainty.

This research contributes to sustainable power system development by enhancing FBMC efficiency, supporting renewable energy integration, and advancing economic welfare in electricity markets. The adaptive GSK framework provides transmission system operators with improved tools for managing cross-border electricity flows while maintaining system security and economic efficiency.

Keywords

Flow-Based Market Coupling, Generation Shift Key, Power Transfer Distribution Factor, Electricity Markets, Optimization, Renewable Energy Integration

Sammanfattning

Denna avhandling handlar om hur man kan förbättra handeln med el mellan olika regioner i Europa. När elmarknaderna blir mer sammanlänkade används en metod som kallas flödesbaserad marknadskoppling (FBMC). Den hjälper till att optimera elhandeln över gränserna och ser till att elnätets kapacitet utnyttjas effektivt. En viktig pusselbit i detta system är något som kallas generation shift key (GSK), som styr hur elproduktionen fördelas på ett smart sätt när förutsättningarna på marknaden ändras. Den här studien undersöker olika metoder för att beräkna dessa GSK-nycklar, eftersom det idag saknas en standardiserad och optimal strategi, vilket är viktigt att utforska vidare.

För att analysera detta har en matematisk modell av elmarknaden och elnätet tagits fram. Modellen simulerar hur elen produceras optimalt, hur marknadskopplingen fungerar och hur systemet balanseras vid oförutsedda händelser. Forskningen har särskilt granskat fem olika strategier för GSK, varav två är nya förslag som utvecklats inom ramen för detta arbete. De nya metoderna är utformade för att vara mer flexibla; en tar hänsyn till att fördelningen inte kan vara negativ, medan den andra tillåter negativa värden för att ge ännu större anpassningsförmåga. Alla dessa strategier har sedan jämförts genom omfattande datorsimuleringar.

Undersökningen baserades på ett modellsystem med tre elområden och analyserades över fyra olika årstider, med både perfekta och mer osäkra prognoser för väder och elkonsumention. Detta för att efterlikna de verkliga variationerna i efterfrågan och tillgång på förnybar energi. Resultaten visar att de nya, föreslagna metoderna för GSK är betydligt mer anpassningsbara än traditionella tekniker. De kan leda till lägre totala driftskostnader för elsystemet och presterar bättre när det gäller att optimera systemets marginalkostnad samt minska behovet av kostsamma justeringar (redispatch) när prognoserna slår fel.

Denna forskning bidrar till utvecklingen av mer hållbara kraftsystem genom att effektivisera den flödesbaserade marknadskopplingen, vilket underlättar integrationen av förnybar energi och kan förbättra den ekonomiska välfärden på elmarknaderna. De anpassningsbara GSK-metoderna ger de som driver transmissionsnäten (systemoperatörerna) bättre verktyg för att hantera elflöden över gränserna på ett säkert och ekonomiskt effektivt sätt.

Nyckelord

Flödesbaserad Marknadskoppling, Generation Shift Key, Överföringsfördelningsfaktor, Elmarknader, Optimering, Integration av Förnybar Energi

Acknowledgments

I would like to express my heartfelt gratitude to everyone who supported and contributed to the completion of my master's thesis. First and foremost, I am deeply thankful to my supervisor, Mohammad Reza Karimi Gharigh, whose guidance and support, despite his demanding schedule, were invaluable throughout this project. I also extend my sincere thanks to my examiner, Mohammad Reza Hesamzadeh, for his insightful input and ideas as well as his expertise in this research. Your contributions have played a significant role in shaping the outcome of this thesis.

I would also like to extend my deepest gratitude to my parents and sister for their unwavering support and encouragement during challenging times, especially when I needed it the most.

My sincere thanks also go to my company, PT. Perusahaan Listrik Negara Persero, for their full support throughout my studies. I hope the knowledge and experience I have gained will contribute meaningfully to the advancement of Indonesia's power system.

Stockholm, October 2025

Johanes Hendra Febrianto Rajagukguk

Contents

| | | |
|----------|--|-----------|
| 1 | Introduction | 1 |
| 1.1 | Background | 1 |
| 1.2 | Problem | 2 |
| 1.2.1 | Original problem and definition | 2 |
| 1.2.2 | Scientific and engineering issues | 2 |
| 1.3 | Purpose | 2 |
| 1.4 | Goals | 3 |
| 1.5 | Research Methodology | 4 |
| 1.6 | Delimitations | 4 |
| 1.7 | Structure of the thesis | 4 |
| 2 | Background | 7 |
| 2.1 | Flow Based Market Coupling (FBMC) | 7 |
| 2.1.1 | The History of The FBMC | 8 |
| 2.1.2 | The FBMC Implementation in Nordic Region | 9 |
| 2.2 | Electricity Market Concepts | 9 |
| 2.2.1 | Optimal Dispatch | 9 |
| 2.2.2 | Marginal Cost | 11 |
| 2.2.3 | Direct Current (DC) Load Flow Model | 12 |
| 2.2.4 | Power Transfer Distribution Functions (PTDF) | 13 |
| 2.3 | The FBMC Process | 14 |
| 2.3.1 | Generation Shift Key | 14 |
| 2.3.2 | Remaining Availability Margin (RAM) | 18 |
| 2.4 | Software | 18 |
| 2.5 | Related Work | 19 |
| 2.6 | Summary | 19 |
| 3 | Methodology | 21 |
| 3.1 | Overview of The Methodology | 21 |

| | | |
|----------|---|-----------|
| 3.2 | Nodal Optimal Power Flow (OPF) | 21 |
| 3.2.1 | Nodal OPF Objective Function | 24 |
| 3.2.2 | Power Balance Constraint | 24 |
| 3.2.3 | Transmission Line Constraint | 24 |
| 3.2.4 | Generation Range Constraint | 25 |
| 3.2.5 | The Nodal OPF Optimization Problem | 26 |
| 3.3 | The Flow-Based Market Coupling (FBMC) Optimization | 26 |
| 3.3.1 | The FBMC Objective Function | 26 |
| 3.3.2 | The FBMC Power Balance Constraint | 27 |
| 3.3.3 | The Remaining Available Margin (RAM) Constraint | 27 |
| 3.3.4 | The Generation Range Constraint | 28 |
| 3.3.5 | The zonal PTDF | 28 |
| 3.3.6 | Generating Shift Key (GSK) | 28 |
| 3.3.6.1 | Proposed GSK | 29 |
| 3.3.7 | The Remaining Available Margin (RAM) | 31 |
| 3.3.8 | The FBMC Optimization Problem | 32 |
| 3.4 | Redispatch | 32 |
| 3.4.1 | The Redispatch Objective Function | 32 |
| 3.4.2 | The Redispatch Power Balance Constraint | 33 |
| 3.4.3 | The Redispatch Transmission Line Constraint | 33 |
| 3.4.4 | The Redispatch Increased and Decreased Power Constraint | 34 |
| 3.4.5 | The Redispatch Generator Range Constraint | 34 |
| 3.4.6 | The Redispatch Optimization Problem | 35 |
| 4 | Case Study | 37 |
| 4.1 | System Model | 37 |
| 4.2 | Implementation | 39 |
| 4.3 | Research Scenarios | 39 |
| 5 | Results and Analysis | 43 |
| 5.1 | Cases and Scenarios Analysis | 43 |
| 5.1.1 | Case 1 | 43 |
| 5.1.2 | Case 2 | 46 |
| 5.1.3 | Case 3 | 48 |
| 5.1.4 | Case 4 | 52 |
| 5.2 | Discussion | 56 |

| | | |
|----------|--|-----------|
| 6 | Conclusions and Future Work | 59 |
| 6.1 | Conclusions | 59 |
| 6.2 | Future work | 60 |
| 6.2.1 | The Power Plant Model and Parameters | 60 |
| 6.2.2 | Running Period Test | 60 |
| 6.2.3 | Data Scope and Scale | 60 |
| 6.3 | Reflections | 61 |
| | References | 63 |

List of Figures

| | | |
|------|--|----|
| 2.1 | Supply and Demand Curve | 11 |
| 2.2 | The FBMC Real-world Process | 15 |
| 2.3 | The FBMC Research Model in General | 16 |
| 3.1 | The Perfect Forecast Procedure | 22 |
| 3.2 | The Imperfect Forecast Procedure | 23 |
| 4.1 | The IEEE 73 bus case study | 38 |
| 5.1 | The Total Cost for the Case 1 Perfect Forecast | 44 |
| 5.2 | The Total Cost for Case 1 Imperfect Forecast | 45 |
| 5.3 | The Redispatch Composition for the Case 1 Perfect Forecast | 45 |
| 5.4 | The Redispatch Composition for the Case 1 Imperfect Forecast | 46 |
| 5.5 | The Case 2 Perfect Forecast | 48 |
| 5.6 | The Case 2 Imperfect Forecast | 50 |
| 5.7 | The Redispatch Composition for the Case 2 Perfect Forecast | 50 |
| 5.8 | The Redispatch Composition Case 2 Imperfect Forecast | 51 |
| 5.9 | The Case 3 Perfect Forecast | 52 |
| 5.10 | The Case 3 Imperfect Forecast | 53 |
| 5.11 | The Redispatch Composition for the Case 3 Perfect Forecast | 54 |
| 5.12 | The Redispatch Composition Case 3 Imperfect Forecast | 54 |
| 5.13 | The Case 4 Perfect Forecast | 55 |
| 5.14 | The Case 4 Imperfect Forecast | 55 |
| 5.15 | The Redispatch Composition for the Case 4 Perfect Forecast | 56 |
| 5.16 | The Redispatch Composition Case 4 Imperfect Forecast | 56 |

List of Tables

| | | |
|-----|---|----|
| 4.1 | The generator types in the system | 41 |
| 4.2 | The Seasonal Load and Renewable Energy Data Range | 42 |
| 4.3 | Case Scenario Load and Renewable Energy Data | 42 |
| 5.1 | The Cost Summary Results in Case 1 for Perfect Forecast | 43 |
| 5.2 | The Cost Summary Results in Case 1 for Imperfect Forecast | 44 |
| 5.3 | The Cost Summary Results in Case 2 for Perfect Forecast | 47 |
| 5.4 | The Cost Summary Results in Case 2 for Imperfect Forecast | 47 |
| 5.5 | The Cost Summary Results in Case 3 for Perfect Forecast | 49 |
| 5.6 | The Cost Summary Results in Case 3 for Imperfect Forecast | 49 |
| 5.7 | The Cost Summary Results in Case 4 for Perfect Forecast | 52 |
| 5.8 | The Cost Summary Results in Case 4 for Imperfect Forecast | 53 |

List of acronyms and abbreviations

| | |
|---------|---|
| AC | alternating current |
| ATC | available transfer capability |
| CBs | critical branches |
| CC | combined cycle |
| CGM | common grid model |
| CNE | critical network element |
| CSP | concentrated solar power |
| CT | combustion turbine |
| CWE | central western europe |
| D-0 | day of operation |
| D-1 | one day before operation day |
| D-2 | two days before operation day |
| DC | direct current |
| ENTSO-E | european network of transmission system operators for electricity |
| EPR | external parallel run |
| EU | european union |
| FAV | final adjustment value |
| FBMC | flow-based market coupling |
| FRM | flow reliability margin |
| GLPK | gnu linear programming kit |
| GSK | generation shift key |
| IEEE | institute of electrical and electronics engineers |
| KKT | karush-kuhn-tucker |
| LP | linear programming |

| | |
|------|---------------------------------------|
| MIP | mixed-integer programming |
| NEMO | nominated electricity market operator |
| NG | natural gas |
| NSFD | non-standard flow direction |
| NWE | north-western europe |
| OPF | optimal power flow |
| PCR | price coupling of regions |
| PTDF | power transfer distribution factor |
| PV | photovoltaic |
| RAM | remaining available margin |
| REN | renewable energy |
| ROR | run-of-river hydro |
| RTPV | rooftop pv |
| SDAC | single day-ahead coupling |
| SDGs | sustainable development goals |
| SFD | standard flow direction |
| SMC | system marginal cost |
| SWE | south-western european |
| TSO | transmission system operator |
| UN | united nations |

Chapter 1

Introduction

1.1 Background

The European Union (EU) plans to fully liberalize the electricity market. This liberalization is based on two principles: an energy-only regional market and market coupling across different regional markets. The mechanism used to couple different electricity markets is called flow-based market coupling (FBMC). The coupling mechanism began in November 2006 in Western European countries. Furthermore, the FBMC has been implemented in the Central Western European (CWE) day-ahead markets [1].

With an increasing number of new energy markets, weather-dependent energy resources, new trading technology, and load demand in the Nordic region, the FBMC method that has been implemented in the CWE region needs to be adapted [2]. Discussions about the FBMC began in 2012 and continued with simulations and reviews through 2020 [3]. This new method has been implemented in the Nordic region since 2021 [4], and FBMC was successfully implemented in Sweden in November 2024 [5].

However, this new method still has plenty of room to be studied and improved in the future. This degree project aims to show and model the FBMC as well as implement it in Python code. The Python code will be used to simulate a case study in a power system. The research also aims to analyze and explore the comparison of the generation shift key (GSK) which is a strategy that has an important role in maximizing the FBMC welfare. The research also presents the new proposed GSK strategies and they will be compared with the existing methods.

1.2 Problem

This section figures the problem related to the flow-based market coupling. The section consists of the problem definition and engineering issues.

1.2.1 Original problem and definition

The flow-based market coupling (FBMC) is a new methodology in the electricity market that is an improvement from the available transfer capability (ATC). The FBMC considers transmission capabilities in the optimization problems compared to the previous method. A critical line within a zone can impact the transfer between areas or zones that have been calculated. This situation is essential to investigate and analyze to improve this new method. In addition to analyzing this situation, a precise capture of the FBMC operation needs to be obtained. In addition to that, the FBMC also found an undecided strategy to calculate the generation shift key (GSK).

1.2.2 Scientific and engineering issues

This degree project mainly focuses on answering the following questions:

- What is the mathematical model of the FBMC method for modeling transmission networks?
- How can the FBMC be modeled and simulated in Python?
- How is the implementation of the proposed GSK strategies?
- How does the proposed GSK strategy compare with the existing strategies?

1.3 Purpose

The purpose of this degree research project is to gain an understanding of FBMC, a new methodology in the electricity market in the European Union (EU). The main aim of the FBMC is to improve the economic welfare of the power system operation in Europe. The FBMC can provide more profit due to transmission capacity transparency [1]. However, this concept still has room to be improved such as the generation shift key (GSK) [6]. And because of that, this research is aimed at the players or participants in the electricity market.

The research provides a mathematical model of the FBMC and figures out how the FBMC operates through a simulation by a Python code. The research project indirectly supports the sustainability of power system operation. The increasing number of the integration of renewable energy into the grid has led the power system market to drive a new methodology. Referring to [6], the FBMC is proposed to solve this situation. This new method is developed to solve previous problems related to congestion management in the transmission. The FBMC is aimed to solve the market problem and increase economic welfare.

This research is related to sustainable goal developments as follows

- Goal 7 (Affordable and Clean Energy)
- Goal 8 (Decent Work and Economic Growth)
- Goal 9 (Industry, Innovation, and Infrastructure)
- Goal 13 (Climate Action)

1.4 Goals

The goal of this project is to provide the concepts of the FBMC through a simulation and to show how the proposed GSK strategy is to be implemented as well as its comparison to the existing methods. This has been divided into the following four sub-goals:

1. Providing a mathematical model of the FBMC
2. Validating the FBMC coupling through a simulation
3. Presenting the implementation of the proposed GSK strategies through a case study
4. Investigating the performance of the proposed GSK strategies in comparison with existing strategies

This project also aims to evaluate how the proposed GSK strategy performs within the FBMC framework, with performance represented by the resulting operational costs and power dispatch outcomes.

1.5 Research Methodology

To answer the research questions in this project, the methodology that will be used is based on experimentation. Prior to the experimentation, a study literature will be done to get insights into how the FBMC is implemented in real-world situations and research that has been done. This literature study is the guidance to design the experimentation. The experiment is built through a simulation using Python code. A case study will be used as the object of the experiment. To obtain a reliable result and prevent a bias when experimenting with the parameters in the system, a random number will be utilized based on the range obtained from the real-world result.

This research project utilizes the main methodology which is arranged based on [7], [8], and [9]. The supporting data for random numbers and parameters will be obtained from the [10] and [11].

1.6 Delimitations

This project has certain delimitations that need to be clearly defined in order to address the research objectives. The delimitations of this thesis project are as follows:

- The case study is limited to the IEEE 73-bus system model.
- Generator cost data is based solely on the IEEE 73-bus system.
- Certain power plant characteristics are omitted to reduce system complexity.
- The load profile does not reflect specific load characteristics or types.
- The study employs an open-source optimization solver.

1.7 Structure of the thesis

This thesis report consists of six chapters. The first chapter introduces the research project by providing a brief background, defining the problem, outlining the delimitations, and stating the goals and purpose of the project. It also explains the foundation of the research methodology used in this study. The second chapter introduces the concept of FBMC and presents the theoretical framework that underpins the research methodology. Additionally,

it describes the general process of the FBMC. Chapter three presents the methodology of the study by applying relevant engineering concepts related to FBMC. It explains how the fundamental theories introduced in Chapter two are adapted to address the research questions. Chapter four provides information about the model used in this research, including the case study and scenarios. Chapter five presents the research results, along with explanations and analysis of the findings. The final chapter, Chapter six, concludes the thesis by summarizing the main outcomes and suggesting potential directions for future research in this area.

Chapter 2

Background

In this chapter, a basic background and theory related to the FBMC are presented. The chapter also provides information related to the history and real-world process of the FBMC. This chapter also describes the software and related work that are used in this research.

2.1 Flow Based Market Coupling (FBMC)

Market coupling is a market design mechanism that aims to efficiently integrate multiple bidding zones by simultaneously optimizing energy trades and the allocation of cross-border transmission capacity. Rather than handling electricity and transmission capacity in separate auctions, market coupling introduces a unified process, using a centralized clearing algorithm to maximize overall social welfare, defined as the sum of consumer surplus, producer surplus, and merchandising surplus [12, 13].

In the European Union (EU), the market coupling is implemented through the single day-ahead coupling (SDAC), coordinated by the European network of transmission system operators for electricity (ENTSO-E). This process relies on the EUPHEMIA algorithm, which takes bids from power exchanges (NEMOs) and capacity constraints from TSOs to compute clearing prices, scheduled cross-border flows, and net positions across zones [14, 15]. A key feature is the use of *implicit auctions*, where transmission capacity is not traded separately, but embedded within the energy trade itself. This removes the need for market participants to reserve cross-border capacity explicitly and results in price convergence across zones [16]. For example, if a surplus of wind power in Germany coincides with higher electricity prices in France, market coupling allows that energy to flow automatically, as long as sufficient grid capacity

exists. This reduces price gaps, improves grid efficiency, and supports the integration of variable renewable energy sources across the continent [17].

According to ENTSO-E, the SDAC now involves 27 countries, 33 TSOs, and 16 NEMOs, handling over 15 million annual trades. The outcomes include significantly reduced price differences, and increased cross-border capacity utilization by over 60% [10].

2.1.1 The History of The FBMC

The process of market integration began in 2006, marked by the initial coupling of electricity markets between France, Belgium, and the Netherlands. A significant milestone occurred in 2014 with the implementation of a common system for calculating day-ahead electricity prices, known as the price coupling of regions (PCR). This system was adopted across much of north-western Europe (NWE), facilitating coordinated price calculation among countries including Belgium, Denmark, Estonia, Finland, France, Germany/Austria, Great Britain, Latvia, Lithuania, Luxembourg, the Netherlands, Norway, Poland, Sweden, Portugal, and Spain. The south-western European (SWE) countries initiated their participation in the PCR framework, thereby aligning their day-ahead market operations with the broader regional integration effort [18].

In May 2015, the flow-based market coupling (FBMC) model was officially implemented in the central western Europe (CWE) region, which includes the Netherlands, Belgium, France, Luxembourg, and Germany. Development of the FBMC methodology by the CWE TSOs began in 2007, followed by two years of offline parallel simulations to evaluate its effectiveness [19].

According to the [19], the FBMC model is derived from the nodal pricing framework, utilizing power transfer distribution factors (PTDF) to estimate power flows. In contrast to full nodal pricing, FBMC applies a zonal or aggregated PTDF matrix to predefined areas or transmission lines, thereby constraining power exchanges between bidding zones. However, this zonal aggregation can result in solutions that remain infeasible in certain parts of the grid, necessitating redispatch measures. Rather than explicitly addressing all individual line constraints, the FBMC approach aims to relax direct restrictions on cross-border trading by concentrating on a subset of transmission elements known as critical branches (CBs), which are most likely to be affected by interzonal power flows.

2.1.2 The FBMC Implementation in Nordic Region

The Nordic region's shift to FBMC started with voluntary efforts by Nordic TSOs in 2012-2013 [20]. This was formalized in 2015 under EU regulations. After regulatory approvals and amendments between 2018 and 2020, internal testing began in 2021, followed by an external parallel run (EPR) in March 2022 [21]. Though briefly paused due to technical issues, the EPR resumed in early 2023 with support from market operators, i.e., NEMOs [22]. Following 15 months of simulations and regulatory endorsement in July 2023 (conditional on improvements), the FBMC successfully launched in the Nordic day-ahead market on October 29, 2024 [23].

2.2 Electricity Market Concepts

In this section, the electricity market concepts related to the research project will be presented. These concepts are underlying the modeling that will later be used to investigate and simulate the FBMC process.

2.2.1 Optimal Dispatch

The main concept that operates the FBMC is the optimal dispatch. According to [24], the optimal dispatch of generation with inelastic demand can be referred to as underlying the optimization concepts. Optimal dispatch refers to the process of minimizing the total cost of electricity generation while fulfilling the required demand. The system operator must ensure that the exact amount of required electricity is supplied at the lowest possible cost.

This is achieved by dispatching generating units in order of increasing marginal cost, starting with the cheapest generators and continuing until the total demand is fulfilled. Each generator has a cost function and capacity limits, and the objective is to satisfy the power balance constraint without exceeding the generator limits.

This concept can be figured through a definition as follows [24]

$$\min \sum_{i=1}^N C_i(Q_i) \quad (2.1)$$

$$\text{subject to } \sum_{i=1}^N Q_i = Q \quad \leftrightarrow \lambda \quad (2.2)$$

$$Q_i \leq K_i \quad \leftrightarrow \mu_i \quad \forall i \quad (2.3)$$

$$Q_i \geq 0 \quad \leftrightarrow \nu_i \quad \forall i \quad (2.4)$$

The C_i represents the cost function of generator i and the output power generation Q_i . The generation output has to fulfill the required demand Q . The output power generation is limited by its capacity which is reflected through its maximum capacity K_i and minimum capacity which can be stated here as zero.

In the equations (2.1)-(2.4), the equation (2.1) depicts the objective function of the optimal dispatch. The equations (2.2)-(2.4) are known as the constraint equations. Based on [24], the symbol \leftrightarrow depicts an association between the constraints with the variables such as λ , μ_i , and ν_i which these variables are known as the Lagrange Multipliers. Solving the equations (2.1)-(2.4) with *Karush–Kuhn–Tucker* (KKT), we can obtain the value for each Lagrange Multiplier variable. These multipliers have a definition as the objective function can be improved with a small change in the constraints. For instance, the λ means a change in the objective function regarding a change in the Q . When a load increases, then the power generation has to be followed to be increased and this situation leads to an increasing cost. How large the cost change is depicted with the λ . This similar meaning also applies to the μ_i and ν_i which means a change or binding with the generation limits can change the objective function of the optimization problem.

The objective function of the optimal dispatch aims to minimize the total cost of generating the power. This total cost means that for each generating electricity at different output levels, the total cost of electricity production over a given interval is the aggregate of the individual cost functions of each power plant which can be presented as follows [24]

$$C(Q_1, Q_2, \dots, Q_N) = \sum_i C_i(Q_i) \quad (2.5)$$

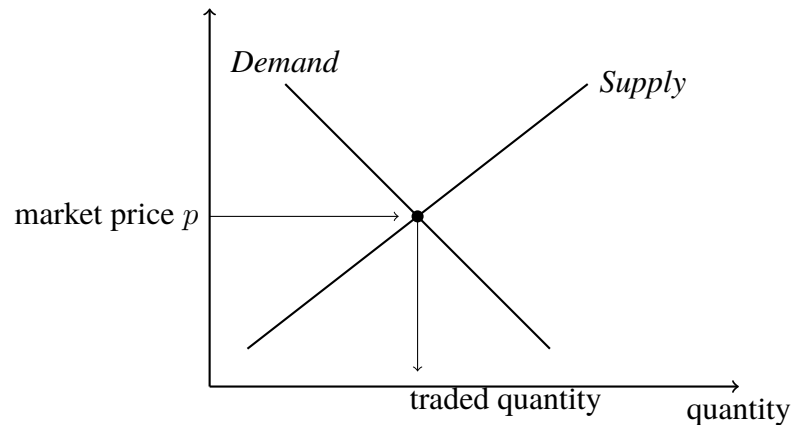


Figure 2.1: Supply and Demand Curve

2.2.2 Marginal Cost

As with any commodity traded in a competitive market, the price of electricity is determined by the interaction of supply and demand. Consider a group of producers, each with known production capacities and associated cost structures. Based on the price at which each producer is willing to supply electricity and their respective production costs, a supply curve can be constructed which can be seen in Figure 2.1.

This curve represents the total quantity of electricity that would be supplied at varying price levels. Similarly, a demand curve can be derived, illustrating the total quantity of electricity consumers are willing to purchase at different prices [25].

This price p can be defined as the marginal cost in the optimal dispatch. According to [24], under the assumption of no network constraints, the optimal dispatch ensures productive efficiency by using the most economical mix of available generators. The marginal cost of the last unit dispatched sets the system price, which serves as a price signal in markets where uniform pricing is applied. This method is fundamental to efficient electricity market operations, ensuring that fixed demand is met in the most cost-effective way.

Based on [24], the KKT of the equations (2.1)-(2.4) can be obtained as follows

$$C'_i(Q_i) = \lambda - \mu_i + \nu_i \quad \forall i \quad (2.6)$$

The common marginal cost, denoted as λ , is referred to as the system marginal cost (SMC), representing the cost of generating one additional unit

of electricity to satisfy an additional unit in demand.

2.2.3 Direct Current (DC) Load Flow Model

In electricity markets, network constraints refer to the physical limitations of the transmission grid that prevent electricity from being transferred freely between different locations. These constraints arise due to factors such as thermal limits on power lines, voltage stability, and system reliability requirements. Even if generation is economically optimal in one area, network constraints may require redispatching to avoid overloading certain transmission lines, which can lead to less efficient but physically feasible solutions.

To define this limitation, we follow the formulation presented in [24], starting with the definition of the net injection of electric power at each node Z_i . This can be expressed as:

$$Z_i = \sum_{l \in U: \text{org}(l)=i} F_l \quad \forall i \quad (2.7)$$

This equation states that the total flow on all lines originating from node i represents the net power flow out of that node, denoted as Z_i . If we consider a bidirectional flow between nodes i and j , and assume negligible losses, then the flow from j to i is equal in magnitude to the flow from i to j , but in the opposite direction. This idea, the net injection at node i can be more accurately written as:

$$Z_i = \sum_{l \in U: \text{org}(l)=i} F_l - \sum_{l \in U: \text{term}(l)=i} F_l \quad (2.8)$$

The $\text{term}(l)$ denotes the terminal node of line l . The principle of power conservation requires that the sum of net injections across all nodes in the network must be zero. This condition is expressed as:

$$\sum_i Z_i = \sum_{l \in U} F_l - \sum_{l \in U} F_l = 0 \quad (2.9)$$

And because of the physical limitations, the power flow over network elements F_l can be defined as follows

$$F_l \leq K_l \quad (2.10)$$

The K_l is the physical limit of the flow in the element l . These concepts provide the foundational elements in the modeling of the FBMC approach, which will be presented later in this research.

To advance the analysis, it is necessary to understand the functions that relate net power injections at each network node to the resulting power flows across transmission elements. Accurately modeling power flows in alternating current (AC) networks involves a relatively complex set of nonlinear equations. Because of that, a simplified approach has been introduced [24]. This approach is called the DC load flow model. A key feature of the DC load flow model is the linearity of its constraint equations relating to the net injections. The DC load flow can be defined as follows

$$F_l = \sum_i PTDF_{l,i} Z_i \quad (2.11)$$

The relation between the net injection at node i and the power flow in the element l is defined by the PTDF $PTDF_{l,i}$.

2.2.4 Power Transfer Distribution Functions (PTDF)

To incorporate these limitations into optimization and market operations, power system engineers use the PTDF [24]. The PTDF is a linear approximation that quantifies how a change in power injection at one bus and withdrawal at another affects the flow on a specific transmission line. This concept tells that a fraction of a transaction between two nodes will flow through each transmission line. These factors are critical for modeling how energy injections (generation) and withdrawals (load) affect the network and are used to formulate the set of feasible power injections that respect all line flow limits.

The PTDF is a matrix element that connects the line l and node i in the system. The matrix consists of the number of $N - 1$ node i times the number of the lines l . This reduction of the number of nodes is a consequence of the energy balance equation and similar to the AC power load flow, the system has to define a reference node or swing node N . Because of this, the choice is limited to the $N-1$. This situation leads to redefined the DC load flow as follows

$$F_l = \sum_{i=1}^{N-1} PTDF_{l,i} Z_i \quad (2.12)$$

2.3 The FBMC Process

In this section, a process of the FBMC will be presented. The process is summarized from [7], [8], and [26]. The FBMC process begins in the days leading up to the day of operation, namely on D-2 (two days ahead), D-1 (one day ahead), and D-0 (the day of operation). On D-2, a nodal optimization is conducted using a base case scenario. This optimization yields several essential parameters for the FBMC process, including the zonal PTDFs, the remaining available margin (RAM), and the generation shift key (GSK). These parameters serve as inputs for the FBMC optimization on D-2. Additionally, any congested transmission lines identified in this step are incorporated as constraints in the FBMC model. The resulting D-2 FBMC optimization provides an initial operational power generation, and this stage also provides the derived RAM and GSK values carried forward as inputs for the D-1 stage.

On D-1, the RAM and GSK may be updated to reflect any changes in power plant availability due to forecast errors or outages, as well as updates in transmission capacity. If such updates occur, a new FBMC optimization is performed, resulting in a revised generation schedule. This step effectively represents the market-clearing process.

On D-0, the system operator manages the real-time operation of the power system. If significant changes occur in renewable generation output and transmission line congestion, the operator may perform a redispatch. This redispatch process uses a nodal optimization approach that accounts for transmission constraints to ensure a secure and economically efficient system operation.

Based on [8], the real-world process of the FBMC can be seen in Figure 2.2. For the research project, adapting a similar model as proposed in [8]. The model is presented in a general flow that can be seen in Figure 2.3

2.3.1 Generation Shift Key

In the FBMC, the matrices serve as fundamental components in determining the outcomes and trading possibilities within the FBMC framework. These matrices are derived using two key inputs: PTDFs and GSKs. PTDFs are based exclusively on the physical characteristics of the power system and indicate how changes in nodal net injections affect line flows. In contrast, GSKs capture the distribution of zonal net position changes across individual nodes, relying on the expertise of the relevant TSO and approximate calculation methodologies [27].

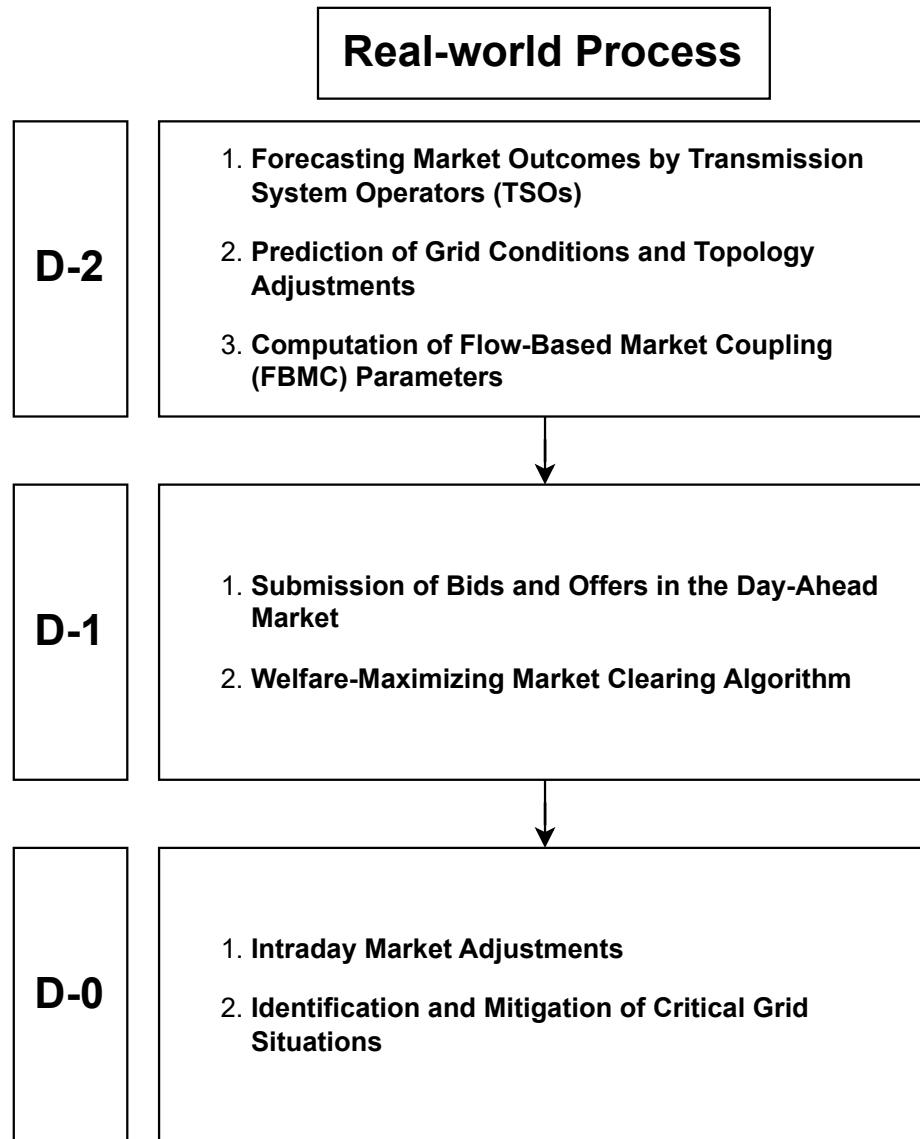


Figure 2.2: The FBMC Real-world Process

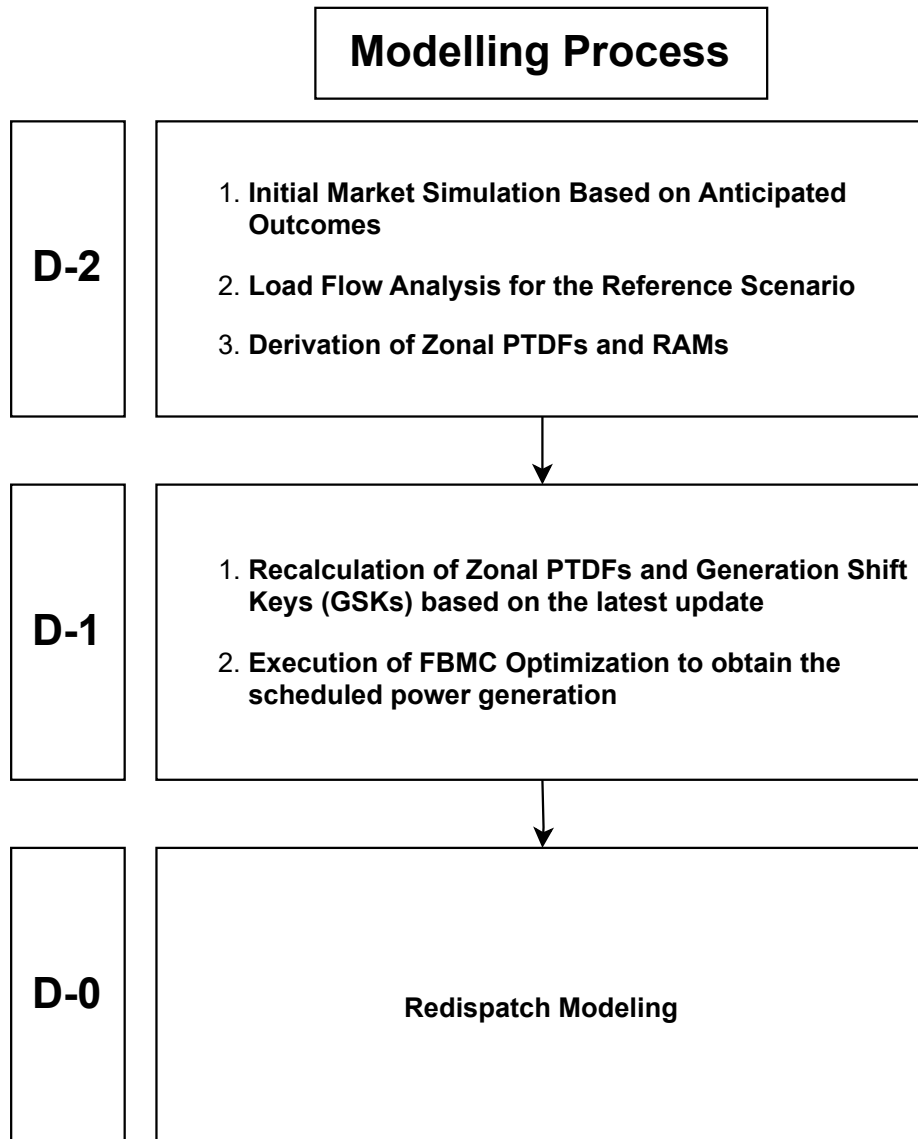


Figure 2.3: The FBMC Research Model in General

The GSKs are essential for translating changes in the net position of a bidding zone into corresponding adjustments in nodal power injections within that zone or into modifications in power flows across interconnections with neighboring zones [28]. Based on [29], a GSK is a method or strategy used to translate changes in the net position of a given bidding zone into estimated increases or decreases in nodal injections within the common grid model (CGM). It provides a zonal-to-nodal mapping that approximates how variations in zonal net demand or supply are distributed across individual generation units within the zone.

Although the GSKs are intended to be defined even prior to the market clearing, in practice, their exact values cannot be determined until the FBMC calculation is finalized. The TSO estimates the GSKs using a "base case" scenario, which reflects anticipated grid topology, zonal net positions, and corresponding power flows for each delivery hour. However, a standardized and precise methodology for determining GSKs remains absent in current operational practice [6].

According to [30], the selection of GSKs has a direct influence on the market equilibrium under the FBMC, and consequently, on resulting electricity prices. Since GSKs affect the zonal PTDFs, their specification plays a critical role in shaping the FBMC outcome. Notably, assigning generation units located far or very far from congested interconnections should not be left to arbitrary decisions by TSOs. Instead, the GSKs should be based on the most accurate generation forecasts available to the TSO.

The other important aspect in the formulation of GSKs is the selection of nodal attributes that serve as the basis for calculating GSK factors. Several approaches are possible, including but not limited to maximum generation or consumption capacity, forecasted generation or consumption from D-2 data, and available excess capacity in the base case scenario [31].

According to [31], when developing a GSK strategy, it is essential to recognize that it represents a linear approximation of an inherently non-linear relationship. Regardless of how market-induced shifts alter the zonal net positions, this linear mapping is assumed to remain valid. Given that generator constraints may not be explicitly incorporated into the chosen method, it is crucial to utilize the most accurate forecast data available when constructing the CGM.

2.3.2 Remaining Availability Margin (RAM)

In the FBMC, two key parameters are used to represent grid constraints in the market optimization process. The first parameter is the zonal PTDF, which quantifies the impact of zonal net position changes on power flows across critical network elements. The second parameter is the RAM, which defines the maximum allowable flow on these elements, accounting for operational security limits and previously reserved capacities [32]. The PTDF matrix and RAM determine the feasibility region (or security domain) at any given point in time [33].

According to [34] and [35], the RAM is defined as follows

$$\sum_{n \in N} PTDF_{(c,n)}^{z2s} \cdot NP_{(n)} \leq RAM_{(c)} \quad \forall c \in C \quad (2.13)$$

The term N defines the set of bidding zones. The $PTDF_{(c,n)}^{z2s}$ defines the zone-to-slack in the PTDF. The term $NP_{(n)}$ depicts the net positions of node n . The term C is the set of line constraints in the flow-based domain.

In this research, the RAM definition that will be used is based on [32], [7], and [8]. The RAM definition can be seen as follows

$$RAM = F_{max} - F'_{ref} - FRM - FAV \quad (2.14)$$

The term F_{max} means the maximum capacity rating in continuous operation for the transmission equipment. The F'_{ref} defines the flow reference based on nodal and zonal calculation. The FRM is the flow reliability margin (FRM). The FRM represents static reductions applied to the RAM and derived from historical observations. They reflect the typical deviations observed between the forecasted base case flows and the actual flows at the point of dispatch for each critical network element (CNE) [26]. The final adjustment values (FAVs) are used to adjust the RAM, either increasing or decreasing the limit range, based on the operational experience of TSOs. These adjustments may account for anticipated remedial actions at the point of dispatch or other complex considerations related to system security and operational reliability [26].

2.4 Software

To simulate the flow-based market coupling process, Python code is utilized to build the model. The model uses the Pyomo and GLPK as its optimization solver. The Pyomo is an open-source optimization modeling language

implemented in Python that provides a versatile framework for formulating, solving, and analyzing a wide range of optimization problems [36]. The GNU linear programming kit (GLPK) is a software package designed to solve large-scale linear programming (LP) and mixed-integer programming (MIP) problems, as well as other related optimization tasks [37].

2.5 Related Work

The research that has been done by [7] and [8] has developed a comprehensive model in the FBMC. This research utilizes concepts that are presented in this research. The methodology presented by this research also has been adapted to this research.

The other research related to the generation shift key (GSK) that was presented by [27] has given insight into how the research of different GSK strategies has been done. The research also shows how the TSOs in Central West European countries operate with different GSK strategies.

The research conducted by [9] gives a deeper insight into how the process of the FBMC operates. The research presents a different point of view of FBMC optimization models which is aligned with the FBMC models presented with [7] and [8]. This research also presents the study case that later will be used in this project research.

2.6 Summary

This chapter provides basic concepts that will be used in this research. The approach from the electricity market point of view has been introduced. The optimal dispatch problem, marginal cost, load flow model, and the matrix PTDF have been presented. This chapter also gives a short insight into the history of the FBMC method. The FBMC process in real-world process was presented as well as the general model of the FBMC process that will be used in this research. The important concepts about the FBMC related to the GSK and the RAM have been presented. The GSK strategies will be explored in this research through the FBMC model process. The other information that was covered in this chapter is related to the software that is used in the research and the related research that has been done.

Chapter 3

Methodology

3.1 Overview of The Methodology

In the next sections, the nodal optimal power flow, the FBMC optimization problem, and the redispatch optimization will be presented. These sections will show how the research defined models that were used in the research. The model is an adaptation of the model that has been shown in Chapter 2 that can be seen in Figure 3.1 and Figure 3.2. This adaptation is done to align the concepts with the research objectivity. In this model, some assumption is applied and ignoring some parameters such as

- Ramp up/ramp down
- Unit commitment
- CO2-free
- Start-up or shutdown time and costs
- Only use a specific time load, not 24 hours or a periodic time

3.2 Nodal Optimal Power Flow (OPF)

In the D-2, the nodal optimal power flow is done to obtain and define the base case study that later will be used in the GSK and RAM calculation. The nodal optimization problem consists of the objective function, the power balance constraints, the transmission limit constraints, and the power generation limits.

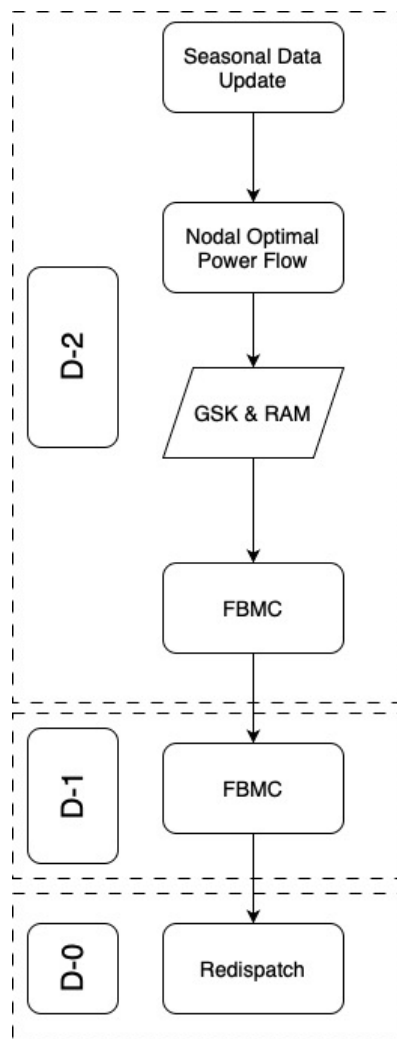


Figure 3.1: The Perfect Forecast Procedure

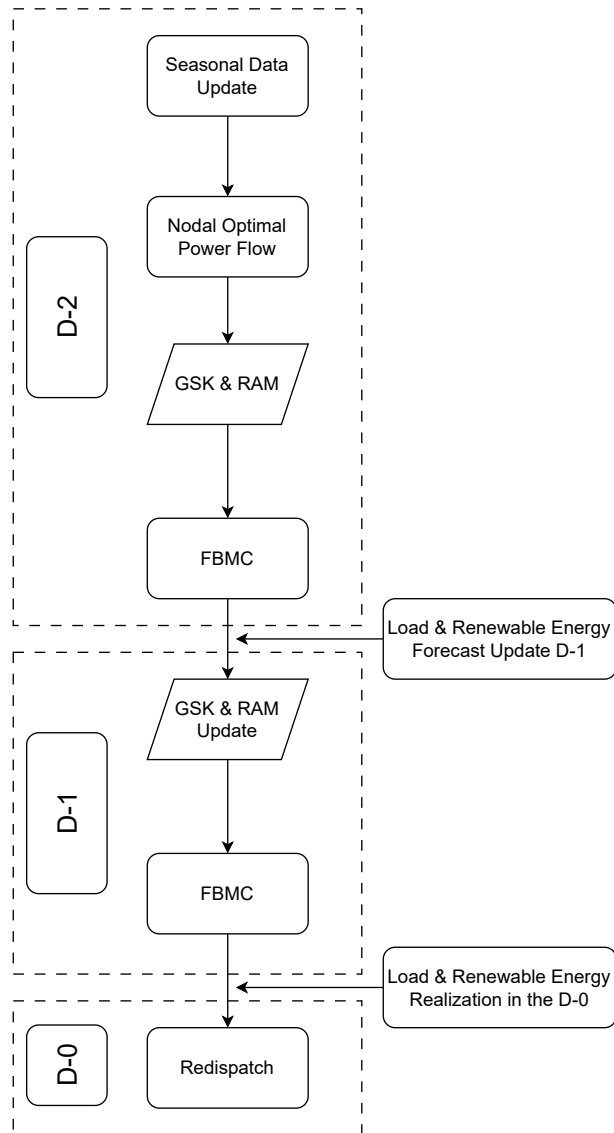


Figure 3.2: The Imperfect Forecast Procedure

3.2.1 Nodal OPF Objective Function

The objective function of the nodal optimization is to gain the most minimal operational cost in the power system operation while fulfilling the limitations stated by the constraints. The objective function definition can be seen as follows

$$\min \sum_{g \in G} costs_g P_g \quad (3.1)$$

The $costs_g$ is a variable cost of a power plant. The data is obtained and defined. This variable cost is defined as a parameter in the code. The P_g is the output power of a power plant which is a result of the optimization.

3.2.2 Power Balance Constraint

To find the solution of the objective function, a power balance constraint is applied to the problem. The power balance constraint defines that the generated output power has to be equal to the required demand in the system. The equation of the power balance constraint can be seen as follows

$$\sum_{d \in D} P_d = \sum_{g \in G} P_g \quad (3.2)$$

The P_d defines the load d that needs to be supplied in the power system and the P_g defines the generated power output from a power plant g . Each demand d belongs to the set of all demands D and every generation g is an element of the set of all generations G .

3.2.3 Transmission Line Constraint

The other constraint in the nodal optimal power flow is the transmission line constraint. This constraint states that a flow in a certain line cannot exceed its maximum capability f_l^{max} . This transmission capability is defined that has two directions because a power flow in the system can flow aligned with the defined direction but sometimes it can flow against its defined direction. The

constraint can be defined as follows

$$\sum_{g \in G} PTDF_{l,g}^G \cdot P_g - \sum_{d \in D} PTDF_{l,d}^D \cdot P_d \leq f_l^{\max} \quad \forall l \in L \quad (3.3)$$

$$\sum_{g \in G} PTDF_{l,g}^G \cdot P_g - \sum_{d \in D} PTDF_{l,d}^D \cdot P_d \geq -f_l^{\max} \quad \forall l \in L \quad (3.4)$$

In this constraint, the matrix PTDF is separated into two matrix PTDF which are load matrix $PTDF_{l,d}^D$ and generation matrix $PTDF_{l,g}^G$. This separation due to mapping the generator and load in the system. This matrix has a similar value to the complete matrix PTDF. The $PTDF_{l,d}^D$ defines the matrix PTDF for the line l and the load that is connected to the bus d . The $PTDF_{l,g}^G$ defines the matrix PTDF for the generator g connected to the bus and the line l . Every line l is an element of the set of all lines L .

3.2.4 Generation Range Constraint

The power generation is constrained to generate power based on their minimum and maximum capacity. This capacity is based on defined information for the IEEE 73 bus study case. In this research, the minimum capacity of power generation is defined as zero. This adjustment is to be done to ensure the system can be optimized for cheaper power plant costs. Stating a minimum generation output restricts a certain power plant from being operated at its minimum capacity. This constraint can be defined as follows

$$P_g \geq P_g^{\min} \quad \forall g \in G \quad (3.5)$$

$$P_g \leq P_g^{\max} \quad \forall g \in G \quad (3.6)$$

The P_g^{\min} defines the minimum power output capacity of a power plant if it connects to the system. The P_g^{\max} is the maximum power output capacity of the power plant if it connects to the system. The optimization tries to solve the problem considering these constraints.

3.2.5 The Nodal OPF Optimization Problem

In this subsection, a complete nodal power flow optimization problem is presented. The optimization problem is as follows

$$\min \sum_{g \in G} costs_g P_g \quad (3.7)$$

$$\text{s.t.} \quad \sum_{g \in G} PTDF_{l,g}^G \cdot P_g - \sum_{d \in D} PTDF_{l,d}^D \cdot P_d \leq f_l^{\max} \quad \forall l \in L \quad (3.8)$$

$$\sum_{g \in G} PTDF_{l,g}^G \cdot P_g - \sum_{d \in D} PTDF_{l,d}^D \cdot P_d \geq -f_l^{\max} \quad \forall l \in L \quad (3.9)$$

$$\sum_{d \in D} P_d = \sum_{g \in G} P_g \quad (3.10)$$

$$P_g \geq P_g^{\min} \quad \forall g \in G \quad (3.11)$$

$$P_g \leq P_g^{\max} \quad \forall g \in G \quad (3.12)$$

3.3 The Flow-Based Market Coupling (FBMC) Optimization

The FBMC optimization can take a process from the D-2 until the day before the operation day (D-1). In general, the FBMC optimization problems have a similar format to the nodal pricing as represented in equations (3.7)-(3.12). To calculate the FBMC optimization, several parameters have to be obtained from the nodal power flow optimization. This section will present the FBMC optimization model including the parameters that construct the FBMC calculation.

3.3.1 The FBMC Objective Function

Similar to the nodal optimal power flow, the FBMC objective function is to obtain the most economic result restricted by defined constraints. The objective function of the FBMC is defined as follows

$$\min \sum_{g \in G} costs_g P_g \quad (3.13)$$

Similar to the nodal optimal power flow, the P_g defines the generated power output from a power plant g and $costs_g$ is the variable cost of the power plant g .

3.3.2 The FBMC Power Balance Constraint

The power balance constraint in the FBMC optimization problem is related to the zones. Each zone has a deviation between the generation output and load demand. This deviation leads to a position of zones that can become an importer or exporter of energy in the power system. This position can be defined as q_z . However, the total of this position in the system has to be equal to zero. This means a balance between the generated power and consumed load. This constraint can be defined as follows

$$q_z = \sum_{i \in I_z} \sum_{g \in G_i} P_g - \sum_{i \in I_z} \sum_{d \in D_i} P_d \quad \forall z \in Z \quad (3.14)$$

$$\sum_{z \in Z} q_z = 0 \quad (3.15)$$

The P_g is the generated output power from an optimized power plant. Generator g belongs to the set of generators G_i that are connected to bus i , where bus i is located in zone z . The variable P_d represents the demand to be supplied in the system. Similar to the generation definition, each demand d is connected to a bus i , which is located within a zone I_z . The demand d is an element of the subset of demands D_i associated with bus i . And each zone z belongs to the set of all zones Z .

3.3.3 The Remaining Available Margin (RAM) Constraint

The other difference in the FBMC compared to the nodal optimal power flow is the presence of the RAM constraint. This constraint states to limit the line based on their remaining available power in the system. This constraint only considers the critical line in its optimization. To calculate this constraint, the zonal PTDF $PTDF_{l,z}^Z$ and the zone net position q_z . The RAM constraint can be defined as follows

$$\sum_{z \in Z} PTDF_{l,z}^Z \cdot q_z \leq RAM_l^{sfd} \quad \forall l \in L^{CNE} \quad (3.16)$$

$$\sum_{z \in Z} PTDF_{l,z}^Z \cdot q_z \geq RAM_l^{nsfd} \quad \forall l \in L^{CNE} \quad (3.17)$$

The RAM_l is the remaining availability margin of a line which included in the critical branch. A deeper explanation of the RAM will be provided in

the next subsections. The RAM in this constraint is divided into two types, standard flow direction (*sfd*) and non-standard flow direction (*nsfd*). The *sfd* defines the normal power-flow direction in the line as well as the *nsfd* depicts the abnormal or reverse situation of the power-flow direction.

3.3.4 The Generation Range Constraint

The generation is limited by its capability. This constraint is similar to the nodal optimal power flow for the generation range. The definition of the generation range constraint can be seen as follows

$$P_g \geq P_g^{\min} \quad \forall g \in G \quad (3.18)$$

$$P_g \leq P_g^{\max} \quad \forall g \in G \quad (3.19)$$

The P_g defines the output power generation by a power plant, and it is restricted by its minimum capability P_g^{\min} and maximum capability P_g^{\max} based on the obtained data.

3.3.5 The zonal PTDF

Translating the nodal pricing into zonal pricing, a variable needs to be defined. The variable is Generating Shift Key (GSK) GSK_i . The GSK transforms the matrix of the nodal PTDF into the zonal PTDF. The equation becomes as follows

$$PTDF_{l,z}^Z = \sum_{i \in I_z} GSK_i \cdot PTDF_{l,i} \quad \text{with} \quad \sum_{i \in I_z} GSK_i = 1 \quad (3.20)$$

in the equations (3.8) and (3.9), the matrix of PTDF is symbolized with $PTDF$ followed by their position as generation g or demand d . Actually, these two matrices PTDF are just a detailed modeling of the nodal matrix PTDF $PTDF_{l,i}$ based on their parts.

3.3.6 Generating Shift Key (GSK)

One of the important components to define an FBMC is a generating shift key (GSK) GSK_i . There are various methods to calculate the GSK. Based on [7], there are generally three methods to calculate the GSK by maximum capacity, by number of nodes in a zone, and by net exports.

Adapting the GSK definition and model that has been defined in the previous chapter, the GSK equations are defined as follows

$$GSK_{i,z} = \frac{\sum_{g \in G_i} P_g^{max}}{\sum_{i \in I_z} \sum_{g \in G_i} P_g^{max}} \quad (3.21)$$

$$GSK_{i,z} = \frac{1}{N_z} \quad (3.22)$$

$$GSK_{i,z} = \frac{q_i^{(e)}}{\sum_{i \in z} q_i^{(e)}} \quad (3.23)$$

In this research, a new GSK calculation method is proposed. This GSK strategy comes from the relation between the line flow, PTDF, and the net export change.

3.3.6.1 Proposed GSK

The proposed GSK idea comes from the DC load Flow (Chapter 2) approach which states the relation between the flow in the line F_l and the net injection at the node q_i . The equation can be seen as follows

$$F_l = \sum_i PTDF_{l,i} \cdot q_i \quad (3.24)$$

The equation (3.24) is the nodal DC load flow and in this research will be rewritten as the actual flow F_{act} . The F_{act} can be defined as follows

$$F_{act} = \sum_i PTDF_{l,i} \cdot q_i \quad (3.25)$$

Because the FBMC works with a zone approach, then the equation (3.24) can be rewritten to align with our modeling in this research as follows

$$F_{app} = \sum_z PTDF_{l,z}^Z \cdot q_z \quad (3.26)$$

The zonal DC power flow is symbolized as approximation flow F_{app} .

Substituting equation (3.20) into equation (3.26) and it can be written as follows

$$F_{app} = \sum_z \sum_{i \in I_z} GSK_i \cdot PTDF_{l,i} \cdot q_z \quad (3.27)$$

The approximation flow F_{app} means how large the electricity flows in the line within the zone.

The proposed method takes a deviation between the actual flow F_{act} and the approximation flow F_{app} . This proposed method aims to find the slightest deviation between the actual and approximated flow. And because of that, it can be defined as follows

$$F_{act} - F_{app} = 0 \quad (3.28)$$

Substituting equation (3.27) into equation (3.28), we obtained as follows

$$F_{act} - \sum_z \sum_{i \in I_z} GSK_i \cdot PTDF_{l,i} \cdot q_z = 0 \quad (3.29)$$

However, the equation (3.29) is a convex function, and to find the optimum solution, we need iteration data which cannot be solved by just a linear equation. Therefore, this equation is need to be converted to become a root mean square. This approach can be seen as follows

$$\left\| F_{act}^{(t)} - \sum_z \sum_{i \in I_z} GSK_i \cdot PTDF_{l,i} \cdot q_z^{(t)} \right\|_2^2 \quad (3.30)$$

To solve the equation (3.30), an iteration has to be done. Because of that, this research uses a number of scenarios T to find the solution to this optimization. This optimization problem can be defined as follows

$$\min_{GSK \in \mathbb{R}^{N \times Z}} \sum_{t=1}^T \left\| F_{act}^{(t)} - F_{app}^{(t)} \right\|_2^2 \quad (3.31)$$

To find the optimal solution to this problem, sets of constraints have to be defined and can be seen as follows

$$\sum_{i \in I_z} GSK_{i,z} = 1 \quad \forall z \in \{1, \dots, Z\} \quad (\text{column sum} = 1) \quad (3.32)$$

$$GSK_{i,z} = 0 \quad \text{if } i \notin I_z \quad (\text{zero-outside-zone}) \quad (3.33)$$

$$F_{app} = \sum_z \sum_{i \in I_z} GSK_i \cdot PTDF_{l,i} \cdot q_z \quad (3.34)$$

The constraints to this optimization are related to the GSK matrix. The first constraint means that the total of the GSK in one zone must be equal to

one. The second constraint is related to the value of GSK node i outside their zone z having to be zero. The second constraint states that the GSK value has to be greater than or equal to zero. And the last constraint states that the F_{app} which depicts the approach zonal flow as stated at the equation (3.27).

3.3.7 The Remaining Available Margin (RAM)

The RAM consists of four elements which are the line capacity C_f , the line load offset $\Delta L_l^{(e)}$, the FRM M_f , and the Final Adjustment Value (FAV) V_f . The RAM is divided into two categories: the standard flow direction (*sfd*) and the non-standard flow direction (*nsfd*).

$$RAM_l^{sfd} = f_l^{\max} - M_f - V_f - \Delta L_l^{(e)} \quad (3.35)$$

$$RAM_l^{nsfd} = -f_l^{\max} + M_f + V_f - \Delta L_l^{(e)} \quad (3.36)$$

The $\Delta L_l^{(e)}$ represents the difference flows on the corresponding lines between the nodal and zonal. The related variable to the base case net exports is $q_i^{(e)}$. The $q_i^{(e)}$ can be defined as follows

$$q_i^{(e)} = g_i^{(e)} - d_i \quad \forall i \in I \quad (3.37)$$

The base case estimates the best situation in the day of the power system. This variable is a result of nodal optimal power flow optimization [9]. The $g_i^{(e)}$ is the generated output power obtained by the nodal optimal power flow and the d_i is the demand at bus i . Because of that, the $\Delta L_l^{(e)}$ calculates the difference between the power flow calculation according to the base case expectation and the power flow calculation according to the base case zonal exports. The base case zonal export $q_z^{(e)}$ is as follows

$$q_z^{(e)} = \sum_{i \in I_z} q_i^{(e)} \quad \forall z \in Z \quad (3.38)$$

This calculation can be written as follows

$$\Delta L_l^{(e)} = \sum_{i \in I} PTDF_{l,i} \cdot q_i^{(e)} - \sum_{z \in Z} PTDF_{l,z}^Z \cdot q_z^{(e)} \quad (3.39)$$

3.3.8 The FBMC Optimization Problem

In this subsection, a complete FBMC optimization problem is presented. The optimization problem is as follows

$$\min \sum_{g \in G} cost_s P_g \quad (3.40)$$

$$\text{s.t.} \quad \sum_{z \in Z} PTDF_{l,z}^Z \cdot q_z \leq RAM_l^{sfd} \quad \forall l \in L^{CNE} \quad (3.41)$$

$$\sum_{z \in Z} PTDF_{l,z}^Z \cdot q_z \geq RAM_l^{nsfd} \quad \forall l \in L^{CNE} \quad (3.42)$$

$$q_z = \sum_{i \in I_z} \sum_{g \in G_i} P_g - \sum_{i \in I_z} \sum_{d \in D_i} P_d \quad \forall z \in Z \quad (3.43)$$

$$\sum_{z \in Z} q_z = 0 \quad (3.44)$$

$$P_g \geq P_g^{\min} \quad \forall g \in G \quad (3.45)$$

$$P_g \leq P_g^{\max} \quad \forall g \in G \quad (3.46)$$

3.4 Redispatch

There is a probability that the feasible solutions to the zonal pricing problems not be aligned with the physical capabilities in the day of operation. Because of that, a generation power output will be required. A redispatching means readjustment of output power generation from a power plant to accommodate the line congestion or changing load demand in the system. Executing a redispatch leads to an additional cost. This additional cost can come from increased costs or decreased costs from a power plant.

In this research project, the redispatch optimization problem which was defined in the [7] and [38] was adapted. The redispatch optimization problems consist of its objective function, transmission line constraint, power balance constraint, increased and decreased power constraint, and generator range constraint.

3.4.1 The Redispatch Objective Function

The objective of the redispatch optimization is to obtain the smallest cost from increasing and decreasing the output power from a power plant in order to fulfill the changes in demand and the power plant as well as the transmission

line limit. This definition can be seen as follows

$$\min \sum_{g \in \mathcal{G}} (C_g^+ \cdot \Delta P_g^+ - K_g^- \cdot \Delta P_g^-) \quad (3.47)$$

This objective function consists of the increased variable cost C_g^+ , the increased output power ΔP_g^+ , the decreased variable cost K_g^- , and the decreased output power ΔP_g^- .

3.4.2 The Redispatch Power Balance Constraint

In this constraint, the increased power output has to be aligned with the decreased power output in the system. This constraint can be defined as follows

$$\sum_{g \in G} (\Delta P_g^+ - \Delta P_g^-) = \Delta P_d \quad \forall g \in G \quad (3.48)$$

This definition depicts that the difference of the ΔP_g^+ and the ΔP_g^- has to be equal to the load deviation. However, there is zero load deviation or perfect demand forecast, that is leads to the difference of the ΔP_g^+ and the ΔP_g^- being equal to zero.

These increased and decreased output power variables also capture the deviations or fluctuations of renewable energy, as represented by the notation for all generation units G .

3.4.3 The Redispatch Transmission Line Constraint

The transmission line constraint in the redispatch optimization has to be adjusted to accommodate the scheduled power generation \bar{P}_g . Because of that, this constraint can be defined as follows

$$\begin{aligned} -f_l^{max} &\leq \sum_{g \in G} PTDF_{l,g}^G \cdot (\bar{P}_g + \Delta P_g^+ - \Delta P_g^-) \\ &\quad - \sum_{d \in D} PTDF_{l,d}^D \cdot P_d \leq f_l^{max} \quad \forall l \in L \end{aligned} \quad (3.49)$$

The scheduled power generation \bar{P}_g is the output generation that has to be declared in the D-1. This value is obtained based on the FBMC process. On the generation side, the power is the summation of the scheduled power, increased output power, and decreased output power.

3.4.4 The Redispatch Increased and Decreased Power Constraint

The other constraint in the redispatch optimization is the presence of a hard restriction to increase the output generation of renewable energy resources. In real-world situations, renewable energy cannot be dispatched to increase its output generation. The possible action to decrease renewable energy power is curtailing their output power. This constraint can be defined as follows

$$\Delta P_g^+ = 0 \quad \forall g \in G^{REN} \quad (3.50)$$

$$\Delta P_g^+ \geq 0 \quad \forall g \in G \quad (3.51)$$

$$\Delta P_g^- \geq 0 \quad \forall g \in G \quad (3.52)$$

The equation (3.50) specifies that there is no possibility to increase the output power from renewable generators G^{REN} . The constraint $\Delta P_g^+ \geq 0$ indicates that the total increase in output power must be nonnegative, while the constraint $\Delta P_g^- \geq 0$ similarly ensures that the decrease in output power cannot take a negative value.

3.4.5 The Redispatch Generator Range Constraint

The generator range in redispatch phase experiences a readjustment. This adjustment includes the scheduled output power \bar{P}_g . Because of that, this constraint can be defined as follows

$$P_g^{min} \leq \bar{P}_g - \Delta P_g^- \quad \forall g \in G \quad (3.53)$$

$$\bar{P}_g + \Delta P_g^+ \leq P_g^{max} \quad \forall g \in G \quad (3.54)$$

The decreased output generation has to consider the scheduled power output and cannot be lower than its minimum power capacity. In this redispatch phase, the minimum output power generation is based on their minimum capacity. This means that if a power plant is scheduled to connect to the grid and needs to be decreased then their output power cannot be lower than its minimum capability. The maximum capability in the redispatch states that the increased power from the scheduled power generation cannot exceed their maximum capability.

3.4.6 The Redispatch Optimization Problem

In this subsection, a complete redispatch optimization problem is presented. The optimization problem is as follows

$$\min \sum_{g \in G} (C_g^+ \cdot \Delta P_g^+ - K_g^- \cdot \Delta P_g^-) \quad (3.55)$$

$$\text{s.t.} \quad \sum_{g \in G} (\Delta P_g^+ - \Delta P_g^-) = \Delta P_d \quad (3.56)$$

$$\begin{aligned} -f_l^{max} &\leq \sum_{g \in G} PTDF_{l,g}^G \cdot (\bar{P}_g + \Delta P_g^+ - \Delta P_g^-) \\ &\quad - \sum_{d \in D} PTDF_{l,d}^D \cdot P_d \leq f_l^{max} \quad \forall l \in L \end{aligned} \quad (3.57)$$

$$P_g^{min} \leq \bar{P}_g - \Delta P_g^- \quad \forall g \in G \quad (3.58)$$

$$\bar{P}_g + \Delta P_g^+ \leq P_g^{max} \quad \forall g \in G \quad (3.59)$$

$$\Delta P_g^+ = 0 \quad \forall g \in G^{REN} \quad (3.60)$$

$$\Delta P_g^+ \geq 0 \quad \forall g \in G \quad (3.61)$$

$$\Delta P_g^- \geq 0 \quad \forall g \in G \quad (3.62)$$

Chapter 4

Case Study

4.1 System Model

In this research, the case study is the RTS-GMLC dataset [39]. This case is a modification and advanced model of the IEEE 73 bus cases. The case has 3 zones that reflect the transaction or transfer between areas. This case is chosen to depict the real-world case scenario where the FBMC is implemented which consists of areas. The case has 73 buses, 120 lines, and 158 generating units. The system case can be seen in Figure 4.1

The types of power plants that are used in this research can be seen in Table 4.1. The dataset is modified to accommodate this study by defining the variable cost, increasing cost, and decremental cost. The research does not include the start-up and shut-down costs. The other cost that is negligible in this research is the charging or discharging cost.

For the power plant energy, the research assumes all of the power plants have unlimited energy resources. The research also neglects the presence of ramp-up and ramp-down speed from the power plants.

From the dataset, the line information that is used in this project is the resistance and reactance. This value is used to calculate the matrix PTDF. The other information from the line information used in this project is the continuous rating. This value reflects the capacity of each transmission line that is operating in this scheme. This rating becomes the input of the capacity C_f that is used in FBMC optimization.

For the bus dataset, the research utilized the load profile to support the analysis and modeling. The other aim of the bus dataset is to give a map of the system to enhance the analysis.

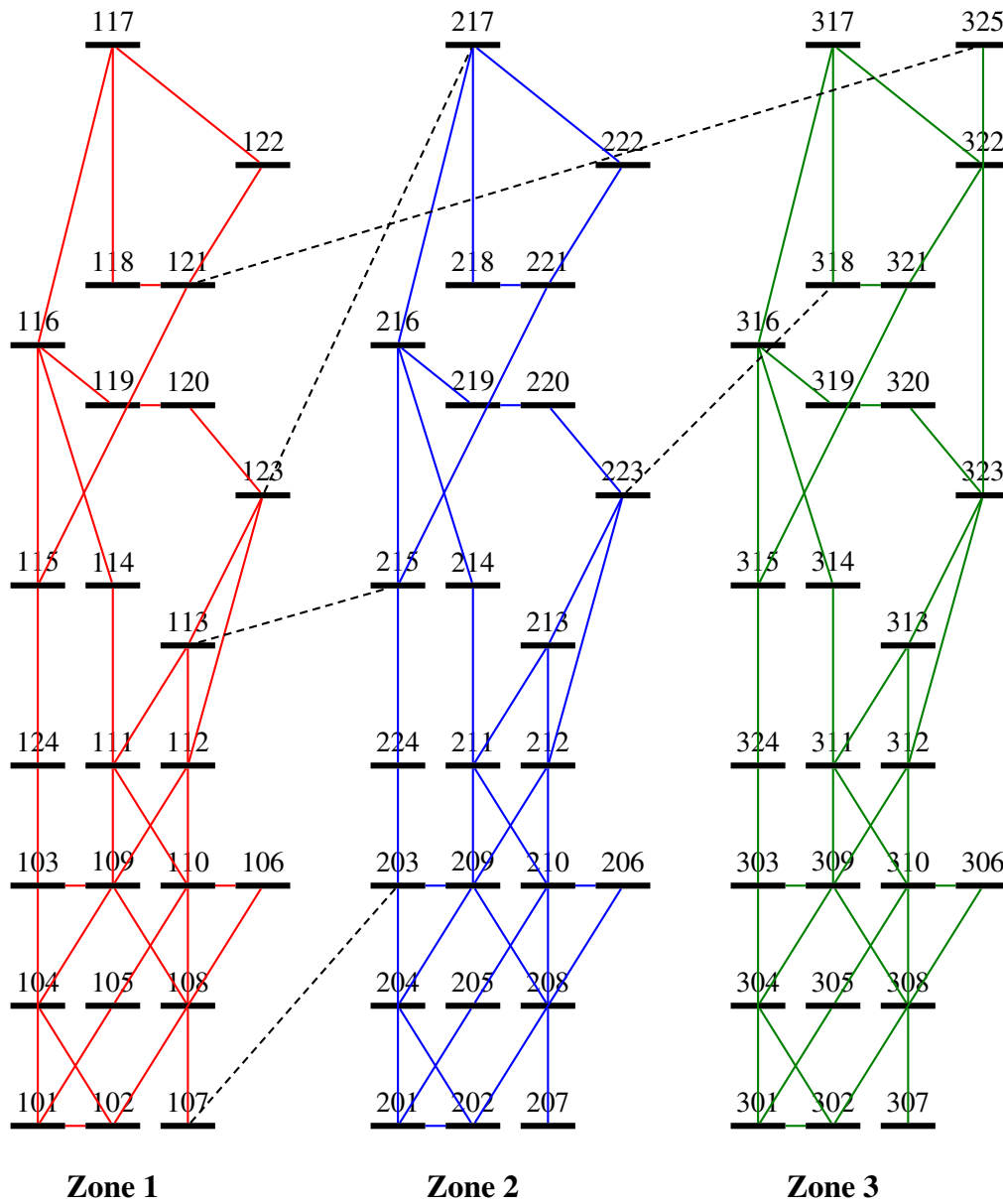


Figure 4.1: The IEEE 73 bus case study

4.2 Implementation

To ensure clear and simple debugging, each GSK calculation and simulation is implemented in a separate Python script. These scripts generally include several components: reading input data, calculating and simulating the nodal power flow, computing the PTDF, GSK, and RAM, scaling the load and renewable energy sources based on given coefficients, simulating the FBMC for Day-2 and Day-1, and performing redispatch simulations. Although these processes are separated into different files, the nodal optimal power flow, PTDF and RAM calculations, and redispatch simulations are generally similar across the scripts. The estimation of GSK values is conducted in dedicated files. This separation is intended to prevent miscalculations and to simplify debugging and parameter adjustment.

4.3 Research Scenarios

In this research, cases, and scenarios will be applied to the simulation in order to obtain a broad perspective and result. This methodology is implemented to reduce the bias in the simulation result. The cases consist of 4 seasons as the FBMC has been implemented in the European countries. Each season has two scenarios for forecasting. The scenarios depict a perfect and an imperfect scenario. This is to give a real-world picture where there is an error in demand and renewable energy resources planning. To decide the cases and scenarios, a random number will be utilized which is implemented into a range based on the obtained data from the real-world realization. The data for the load and renewable generation realization are obtained from the Svenska kraftnät [11]. The statistics that will be used in this research came from a realization in 2024. For the forecast error, the load and renewable forecast data are obtained from the ENTSO-E [10] for Sweden in 2024 which is a similar year to the realization from the Svenska kraftnät data. To get the coefficient for load and renewable generation for each season, this research utilizes a normalization method [40]. To implement this method, first, the peak load and total generation for renewable energy resources was chosen. After that, the data for load and renewable energy was separated based on the seasons. For each season, the minimum value and highest value are decided. These minimum and maximum values were divided by the peak or maximum value in one year. Based on this procedure, the load data and renewable generation data range can be seen in Table 4.2

To obtain the forecast error range, the data will be processed with a similar normalization procedure. However, to reduce the inconsistency and bias, a year-scale was used to decide the range for forecast error. The range for forecast error is as follows

- Load: 0.841 - 1.12
- Renewable Energy: 0.641 - 1.548

The forecast error coefficient used in this research can be seen in Table 4.3. In this simulation, all of the cases only reflect a certain time in one day. The other assumption used in this research is that the critical network element was chosen based on the 5% rule. This rule is subtracted from any two zonal PTDFs of a line, and if it exceeds 5%, the line is considered to be a critical branch [41].

Table 4.1: The generator types in the system

| Generator Type | Number of Units | Brief Description |
|-----------------------------------|------------------------|--|
| CT (Combustion Turbine) | 39 | Simple gas turbine, fast response, medium efficiency |
| RTPV (Rooftop PV) | 31 | Rooftop photovoltaic panels, small-scale installations |
| PV (Photovoltaic) | 25 | Large-scale solar photovoltaic power plant |
| STEAM | 23 | Steam-driven plant, typically coal- or gas-fired |
| HYDRO | 19 | Hydroelectric power plant |
| CC (Combined Cycle) | 10 | Combined gas-and-steam cycle, high efficiency |
| WIND | 4 | Wind turbine power plant |
| SYNC_COND (Synchronous Condenser) | 3 | No active power output; used for voltage support |
| NUCLEAR | 1 | Nuclear power plant |
| ROR (Run-of-River Hydro) | 1 | River-flow hydro plant, output depends on river flow |
| CSP (Concentrated Solar Power) | 1 | Solar thermal plant using mirrors/lenses to concentrate heat |
| STORAGE | 1 | Energy storage system |

Table 4.2: The Seasonal Load and Renewable Energy Data Range

| Seasons | Load | | Renewable Energy | |
|---------|---------|---------|------------------|---------|
| | Minimum | Maximum | Minimum | Maximum |
| Spring | 0.510 | 0.789 | 0.467 | 0.919 |
| Summer | 0.460 | 0.619 | 0.380 | 0.803 |
| Fall | 0.526 | 0.778 | 0.469 | 0.940 |
| Winter | 0.687 | 1.000 | 0.625 | 1.000 |

Table 4.3: Case Scenario Load and Renewable Energy Data

| Case | Scenario | Day | Load | | | Renewable Energy | | |
|--------|-----------|-----|--------|--------|--------|------------------|--------|--------|
| | | | Zone 1 | Zone 2 | Zone 3 | Zone 1 | Zone 2 | Zone 3 |
| Spring | Perfect | D-1 | 1 | 1 | 1 | 1 | 1 | 1 |
| | | D-0 | 1 | 1 | 1 | 1 | 1 | 1 |
| | Imperfect | D-1 | 1.036 | 0.899 | 0.92 | 1.01 | 0.801 | 1.44 |
| | | D-0 | 1.001 | 0.939 | 1.106 | 1.188 | 0.788 | 0.961 |
| Summer | Perfect | D-1 | 1 | 1 | 1 | 1 | 1 | 1 |
| | | D-0 | 1 | 1 | 1 | 1 | 1 | 1 |
| | Imperfect | D-1 | 0.984 | 1.036 | 1.067 | 0.789 | 1.199 | 1.381 |
| | | D-0 | 1.016 | 1.071 | 0.931 | 1.262 | 1.352 | 0.989 |
| Fall | Perfect | D-1 | 1 | 1 | 1 | 1 | 1 | 1 |
| | | D-0 | 1 | 1 | 1 | 1 | 1 | 1 |
| | Imperfect | D-1 | 0.867 | 0.923 | 0.899 | 1.163 | 0.828 | 0.89 |
| | | D-0 | 0.998 | 1.044 | 1.072 | 1.109 | 0.931 | 1.066 |
| Winter | Perfect | D-1 | 1 | 1 | 1 | 1 | 1 | 1 |
| | | D-0 | 1 | 1 | 1 | 1 | 1 | 1 |
| | Imperfect | D-1 | 0.932 | 0.97 | 0.915 | 1.46 | 1.222 | 0.736 |
| | | D-0 | 1.045 | 1.118 | 0.955 | 1.102 | 1.415 | 1.123 |

Chapter 5

Results and Analysis

5.1 Cases and Scenarios Analysis

In this section, the results and analysis of the scenarios and cases will be shown. The section will be divided into two main scenarios that reflect the perfect and imperfect of forecasting the load and renewable energy resources. For the second scenario, the seasons will be delivered in cases. The GSK strategies will be symbolized as GSK 1 for the capability, GSK 2 for the average node, GSK 3 for the net export, GSK 4 for the proposed GSK strategy.

5.1.1 Case 1

In this case, we obtained the result for the perfect forecast that can be seen in Table 5.1 and for the imperfect forecast in the Table 5.2. The data shows that during the perfect forecast the GSK 1 obtains the lowest cost in the FBMC

Table 5.1: The Cost Summary Results in Case 1 for Perfect Forecast

| | GSK 1 | GSK 2 | GSK 3 | GSK 4 |
|--|-----------|-----------|-----------|-----------|
| Total Operational Cost Nodal OPF (\$) | 54009.074 | 54009.074 | 54009.074 | 54009.074 |
| System Marginal Cost Nodal OPF (\$/MWh) | 25.873 | 25.873 | 25.873 | 25.873 |
| Total Operational Cost FBMC D-2 (\$) | 44613.679 | 46885.796 | 47605.135 | 47605.135 |
| System Marginal Cost FBMC D-2 (\$/MWh) | 21.713 | 35.822 | 27.796 | 42.083 |
| Total Operational Cost FBMC D-1 (\$) | 44613.679 | 46885.796 | 47605.135 | 47605.135 |
| System Marginal Cost FBMC D-1 (\$/MWh) | 21.713 | 35.822 | 27.796 | 42.083 |
| Total Operational Cost Redispatch (\$) | 17632.695 | 15939.379 | 18308.929 | 17307.251 |
| System Marginal Cost Redispatch (\$/MWh) | 46.878 | 46.878 | 46.371 | 46.314 |

Table 5.2: The Cost Summary Results in Case 1 for Imperfect Forecast

| | GSK 1 | GSK 2 | GSK 3 | GSK 4 |
|--|--------------|--------------|--------------|--------------|
| Total Operational Cost Nodal OPF (\$) | 54009.074 | 54009.074 | 54009.074 | 54009.074 |
| System Marginal Cost Nodal OPF (\$/MWh) | 25.873 | 25.873 | 25.873 | 25.873 |
| Total Operational Cost FBMC D-2 (\$) | 44613.679 | 46885.796 | 47605.135 | 47605.135 |
| System Marginal Cost FBMC D-2 (\$/MWh) | 21.713 | 35.822 | 27.796 | 42.083 |
| Total Operational Cost FBMC D-1 (\$) | 35999.781 | 35999.781 | 32200.598 | 35999.781 |
| System Marginal Cost FBMC D-1 (\$/MWh) | 25.736 | 21.609 | 23.314 | 21.609 |
| Total Operational Cost Redispatch (\$) | 30792.164 | 30792.164 | 37648.496 | 30792.164 |
| System Marginal Cost Redispatch (\$/MWh) | 48.598 | 48.598 | 48.918 | 48.598 |

optimization. In this result, we can see that the GSK 4 have a result close to the GSK 3 which assigns an net export to the nodes.

In the imperfect scenario, the load and renewable energy resources error forecasting lead to cost changes in the FBMC D-1 and redispatch. In the FBMC D-1, the GSK 3 obtains the lowest cost compared to others. This result is not followed by the system marginal cost which in the D-1, the GSK 4 and 2 obtain the lowest system marginal cost. An unexpected shift occurs in the total cost for redispatch where the GSK 3 obtains the highest cost. The result shows that GSK 1,2, and 4 obtain a similar result for the total operational cost. The result also shows a similar situation with the system marginal cost for redispatch which GSK 3 shows the highest cost while the others obtain similar costs.

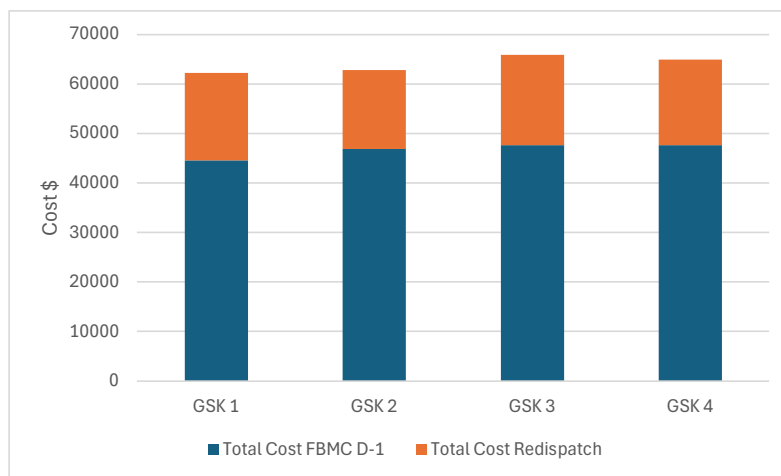


Figure 5.1: The Total Cost for the Case 1 Perfect Forecast

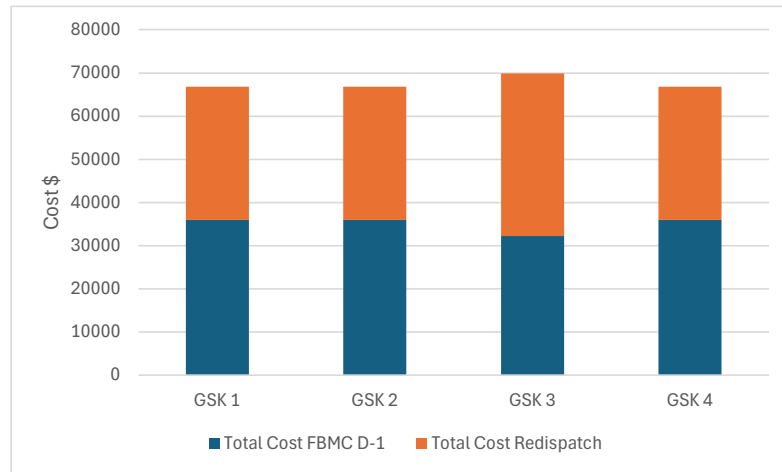


Figure 5.2: The Total Cost for Case 1 Imperfect Forecast

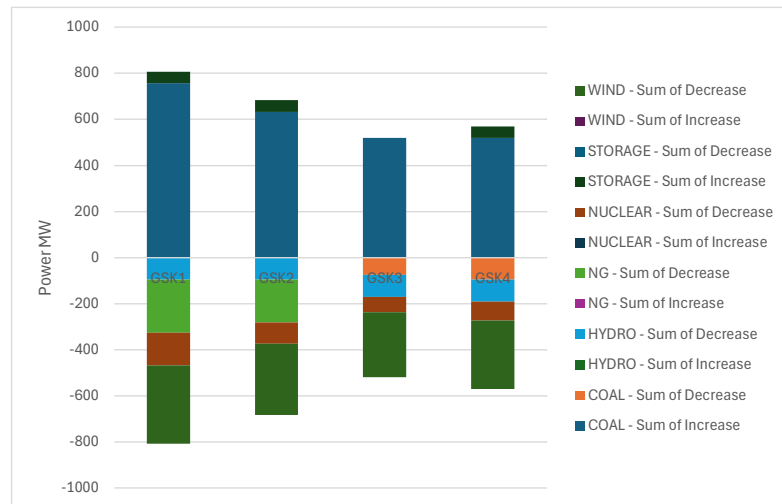


Figure 5.3: The Redispatch Composition for the Case 1 Perfect Forecast

Based on the obtained result in the total cost for the case 1 with perfect scenario Figure 5.1, we can see that the GSK 1,2, and 4 obtain similar results with \$ 66791.944. The GSK 3 shows a higher total cost compared to the others with \$ 69849.094. For the imperfect scenario, the total cost result can be seen in Figure 5.2.

The redispatch result for this case in perfect forecast can be seen in Figure 5.3. The proposed GSK, the GSK 4, shows a total increase and total decrease are 569.282 MW, respectively. The result shows that the GSK 3 obtains the lowest power needed to be redispatched with 519.282 MW.

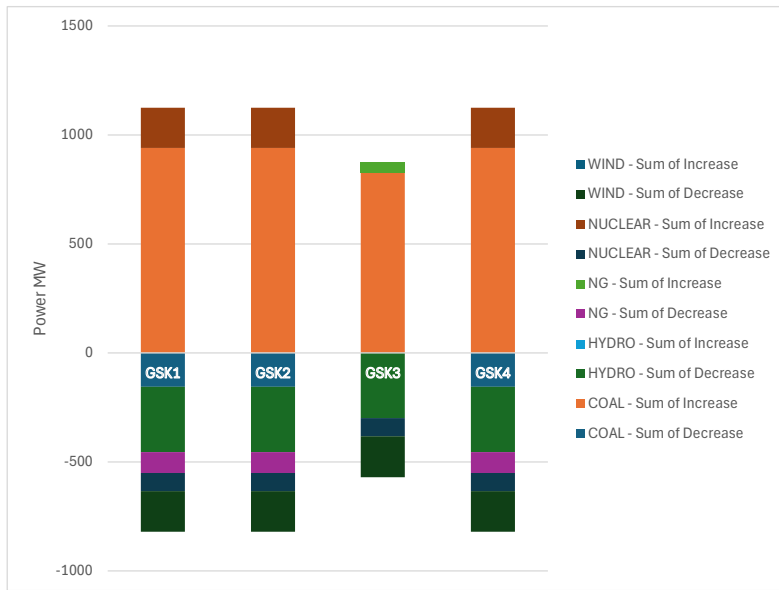


Figure 5.4: The Redispatch Composition for the Case 1 Imperfect Forecast

However, this result contradicts with the high cost spent by this GSK because it is preferred to decrease the coal power plant which has high variable decrease cost.

In the imperfect scenario, the result of redispatch can be seen in Figure 5.4. The GSK 3 obtains the lowest total power to be increased and decreased compared to the other methods. In GSK 3, the natural gas (NG) power plant is preferred to be increased which leads to the cost of redispatch in GSK 3 being the highest spending cost compared to the other GSK strategies.

5.1.2 Case 2

This case reflects the summer situation where the load profile is the lowest period in one year. The summary result for the perfect forecast can be seen in Table 5.3 and for the imperfect forecast in Table 5.4

This case reflects the lowest demand in the season. In the perfect scenario, all of the GSKs show a similar result for the nodal optimal power flow, FBMC, and the redispatch. However, for the system marginal cost, it shows that the GSK 3 obtained the lowest cost. For the proposed GSK, the GSK 4 obtains a similar cost to the GSK 2 with 8.528 \$/MWh. This result also indicates that the GSK 4 and 2 are the second cheapest cost compared to other methods.

In the imperfect scenario, a deviation in the load and renewable resources has led to a changing cost for all of the GSK from the D-1 and the redispatch.

Table 5.3: The Cost Summary Results in Case 2 for Perfect Forecast

| | GSK 1 | GSK 2 | GSK 3 | GSK 4 |
|--|--------------|--------------|--------------|--------------|
| Total Cost Nodal OPF (\$) | 1939.380 | 1939.380 | 1939.380 | 1939.380 |
| System Marginal Cost Nodal OPF (\$/MWh) | 10.514 | 10.514 | 10.514 | 10.514 |
| Total Cost FBMC D-2 (\$) | 1939.380 | 1939.380 | 1939.380 | 1939.380 |
| System Marginal Cost FBMC D-2 (\$/MWh) | 8.937 | 8.528 | 2.810 | 8.528 |
| Total Cost FBMC D-1 (\$) | 1939.380 | 1939.380 | 1939.380 | 1939.380 |
| System Marginal Cost FBMC D-1 (\$/MWh) | 8.937 | 8.528 | 2.810 | 8.528 |
| Total Cost Redispatch (\$) | 685.304 | 685.304 | 685.304 | 685.304 |
| System Marginal Cost Redispatch (\$/MWh) | 20.652 | 20.652 | 20.652 | 20.652 |

Table 5.4: The Cost Summary Results in Case 2 for Imperfect Forecast

| | GSK 1 | GSK 2 | GSK 3 | GSK 4 |
|--|--------------|--------------|--------------|--------------|
| Total Cost Nodal OPF (\$) | 1939.380 | 1939.380 | 1939.380 | 1939.380 |
| System Marginal Cost Nodal OPF (\$/MWh) | 10.514 | 10.514 | 10.514 | 10.514 |
| Total Cost FBMC D-2 (\$) | 1939.380 | 1939.380 | 1939.380 | 1939.380 |
| System Marginal Cost FBMC D-2 (\$/MWh) | 8.937 | 8.528 | 2.810 | 8.528 |
| Total Cost FBMC D-1 (\$) | 2084.781 | 2078.895 | 2005.673 | 2078.895 |
| System Marginal Cost FBMC D-1 (\$/MWh) | 8.937 | 8.528 | 2.810 | 8.528 |
| Total Cost Redispatch (\$) | 2085.263 | 2096.484 | 2236.068 | 2096.484 |
| System Marginal Cost Redispatch (\$/MWh) | 20.652 | 20.652 | 20.652 | 20.652 |

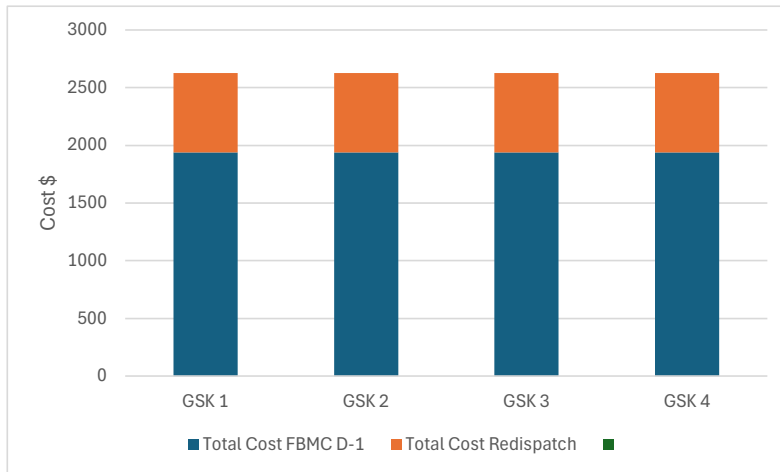


Figure 5.5: The Case 2 Perfect Forecast

In the FBMC D-1, all of the GSKs increase the total cost. The GSK 3 obtained the lowest cost compared to others. This position is followed by the GSK 4 and 2. However, in the redispatch stage, the GSK 1 obtains the lowest cost, and the GSK 3 becomes the highest cost. In this stage, the GSK 4 becomes the second lowest cost with \$ 2096.484.

The total cost for the case 2 with a perfect forecast can be seen in Figure 5.5. The result shows that all of the GSK strategies obtain a similar result. However, in the scenario imperfect forecast that can be seen in Figure 5.6, there a different results within each other. The GSK 1 becomes the lowest total cost with \$ 4170.044 in this scenario. The GSK 4 obtained a cheaper cost compared to the GSK 3 with a difference of about \$66.361.

The redispatch outcome for this case under the perfect forecast scenario is illustrated in Figure 5.7. This graph shows that all of the GSK strategies obtained a similar result with the power plant that needs to be redispatched. However, when it comes to the imperfect forecast scenario, the total power that needs to be redispatched for each GSK becomes different. The result can be seen in Figure 5.8. In this graph, the GSK 3 shows the largest total increasing and decreasing power. For the proposed GSK strategies, they obtain a total power needed to be increased by around 193.457 MW and decreased power by around 156.287 MW.

5.1.3 Case 3

In this case, the system reflects the spring season. The result for the perfect forecast can be seen in Table 5.5 and for the imperfect forecast in Table 5.6

Table 5.5: The Cost Summary Results in Case 3 for Perfect Forecast

| | GSK 1 | GSK 2 | GSK 3 | GSK 4 |
|--|--------------|--------------|--------------|--------------|
| Total Cost Nodal OPF (\$) | 26588.759 | 26588.759 | 26588.759 | 26588.759 |
| System Marginal Cost Nodal OPF (\$/MWh) | 24.093 | 24.093 | 24.093 | 24.093 |
| Total Cost FBMC D-2 (\$) | 24203.899 | 23619.840 | 22931.709 | 23619.840 |
| System Marginal Cost FBMC D-2 (\$/MWh) | 28.988 | 17.727 | 23.190 | 17.727 |
| Total Cost FBMC D-1 (\$) | 24203.899 | 23619.840 | 22931.709 | 23619.840 |
| System Marginal Cost FBMC D-1 (\$/MWh) | 28.988 | 17.727 | 23.190 | 17.727 |
| Total Cost Redispatch (\$) | 3258.443 | 4119.960 | 5210.855 | 4119.960 |
| System Marginal Cost Redispatch (\$/MWh) | 39.197 | 39.197 | 39.197 | 39.197 |

Table 5.6: The Cost Summary Results in Case 3 for Imperfect Forecast

| | GSK 1 | GSK 2 | GSK 3 | GSK 4 |
|--|--------------|--------------|--------------|--------------|
| Total Cost Nodal OPF (\$) | 26588.76 | 26588.76 | 26588.76 | 26588.76 |
| System Marginal Cost Nodal OPF (\$/MWh) | 24.09 | 24.09 | 24.09 | 24.09 |
| Total Cost FBMC D-2 (\$) | 24203.899 | 23619.840 | 22931.709 | 23619.840 |
| System Marginal Cost FBMC D-2 (\$/MWh) | 23.813 | 17.727 | 23.190 | 17.727 |
| Total Cost FBMC D-1 (\$) | 20934.402 | 20886.818 | 20465.589 | 20886.818 |
| System Marginal Cost FBMC D-1 (\$/MWh) | 28.988 | 16.803 | 21.317 | 16.803 |
| Total Cost Redispatch (\$) | 4688.54772 | 4855.851 | 7567.155 | 4855.851 |
| System Marginal Cost Redispatch (\$/MWh) | 44.419 | 44.419 | 42.537 | 44.419 |

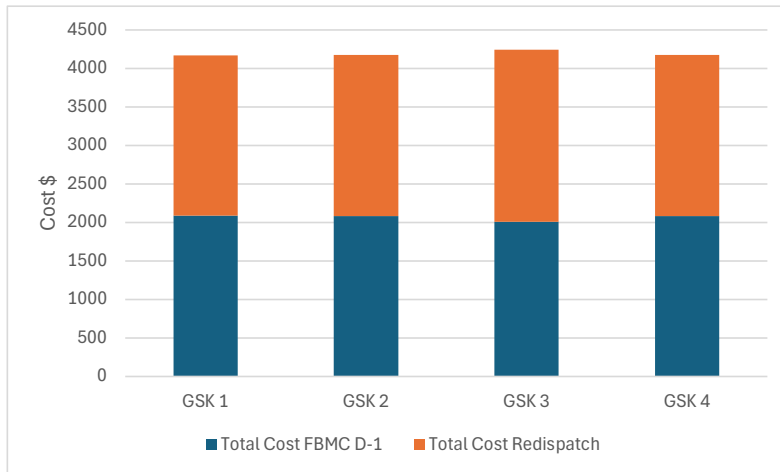


Figure 5.6: The Case 2 Imperfect Forecast

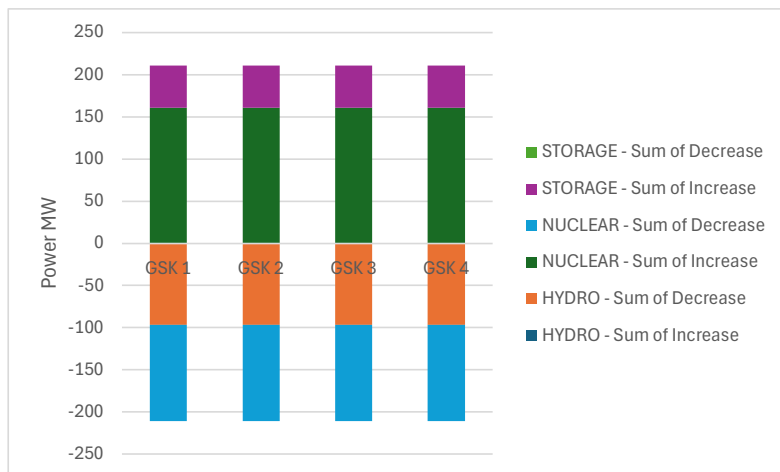


Figure 5.7: The Redispatch Composition for the Case 2 Perfect Forecast

The cost summary table shows that in the perfect forecast, the GSK 2 and 4 obtained the lowest cost in the FBMC D-2 as well as in the D-1. For the system marginal cost, the GSK 2 and 4 are the lowest cost followed by the GSK 3. In the redispatch, all of the GSK strategies obtain a similar result for the system marginal cost.

The result for the imperfect scenario in this case shows that there is a decrease in the cost in the FBMC D-1. The GSK 3 obtains the lowest cost compared to the others. However, for the system marginal cost for the FBMC D-1, the GSK 2 and 4 have similar results and a lower cost compared to the GSK 1 and 3. In the redispatch stage, the GSK 1 obtains the lowest cost

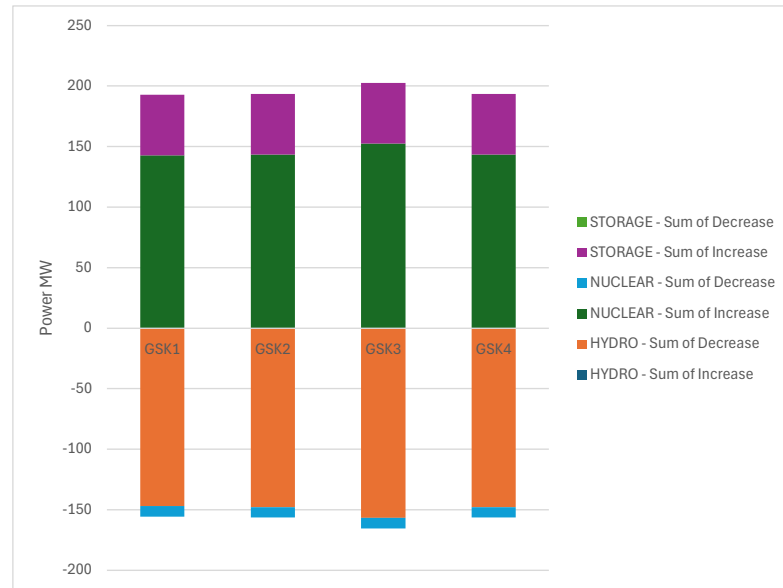


Figure 5.8: The Redispatch Composition Case 2 Imperfect Forecast

compared to the others. The GSK 4 obtains a similar result to the GSK 2. However, the system marginal cost shows that the system marginal cost for the GSK 3 has the lowest cost with 42.54 \$/MWh compared to the others which have similar results with 44.42 \$/MWh.

As the total cost for the perfect scenario can be seen in the Figure 5.9, the total cost for the GSK 1 is the lowest cost compared to the others. The GSK 4 obtained a similar result with the GSK 2 with \$27739.801.

The total cost result in the FBMC and redispatch for the imperfect forecast can be seen in Figure 5.10. The graph shows that GSK 1 obtains the lowest total cost compared to the others. This result is similar to the perfect scenario. The GSK 4 obtains a similar result to the GSK 2 about \$25742.669. This result is lower compared to the GSK 3 which obtained around \$28032.744.

Under perfect forecasting conditions, the redispatch result for this case is depicted in Figure 5.11. The graph depicts a result where the GSK 2 and 4 obtain a similar total power that needs to be redispatched with the increased and decreased power around 419.224 MW, respectively. This result is the lowest total power compared to the others. The GSK 1 and 5 obtained different results that require increased and decreased power and they obtained a larger power compared to the GSK 2 and 4.

The result of redispatch in the imperfect scenario can be observed in Figure 5.12. The outcome reveals that the GSK 3 obtains the lowest total redispatched power around 578 MW for the increased power and 371.607 MW

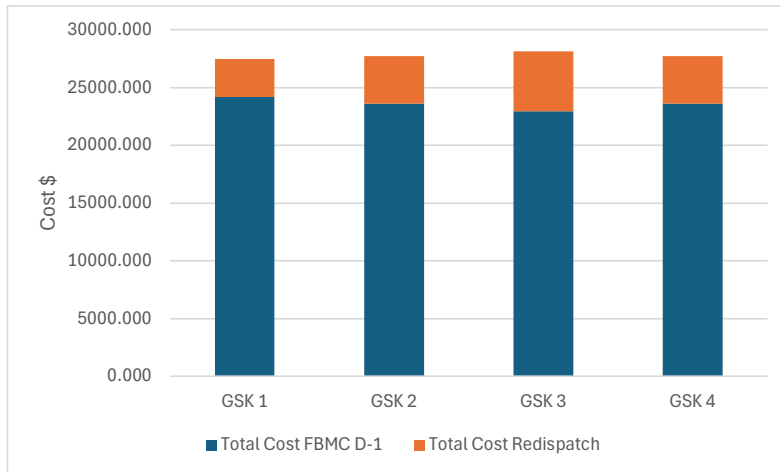


Figure 5.9: The Case 3 Perfect Forecast

Table 5.7: The Cost Summary Results in Case 4 for Perfect Forecast

| | GSK 1 | GSK 2 | GSK 3 | GSK 4 |
|--|-----------|-----------|-----------|-----------|
| Total Cost Nodal OPF (\$) | 32805.832 | 32805.832 | 32805.832 | 32805.832 |
| System Marginal Cost Nodal OPF (\$/MWh) | 24.097 | 24.097 | 24.097 | 24.097 |
| Total Cost FBMC D-2 (\$) | 31548.657 | 33356.535 | 34932.306 | 34932.306 |
| System Marginal Cost FBMC D-2 (\$/MWh) | 24.011 | 31.532 | 25.858 | 24.539 |
| Total Cost FBMC D-1 (\$) | 31548.657 | 33356.535 | 34932.306 | 34932.306 |
| System Marginal Cost FBMC D-1 (\$/MWh) | 24.011 | 31.532 | 25.858 | 24.539 |
| Total Cost Redispatch (\$) | 11254.877 | 8440.019 | 8959.468 | 7904.863 |
| System Marginal Cost Redispatch (\$/MWh) | 43.131 | 43.500 | 43.500 | 43.500 |

for the decreased power.

5.1.4 Case 4

This case reflects the fall season where the summary result for the perfect forecast can be seen in Table 5.7 and for the imperfect forecast in Table 5.8

The cost summary for this scenario shows that the GSK 1 obtains the lowest cost and is followed by the GSK 2 in the second position with \$33356.535. The GSK obtains the second lowest cost for the system marginal cost with 24.539 \$/MWh. In the redispatch, the GSK 4 obtained the lowest operational cost compared to the others.

In the imperfect forecast, the GSK 4 also shows a better result for the total operational cost in the FBMC D-1. This result is also followed by their

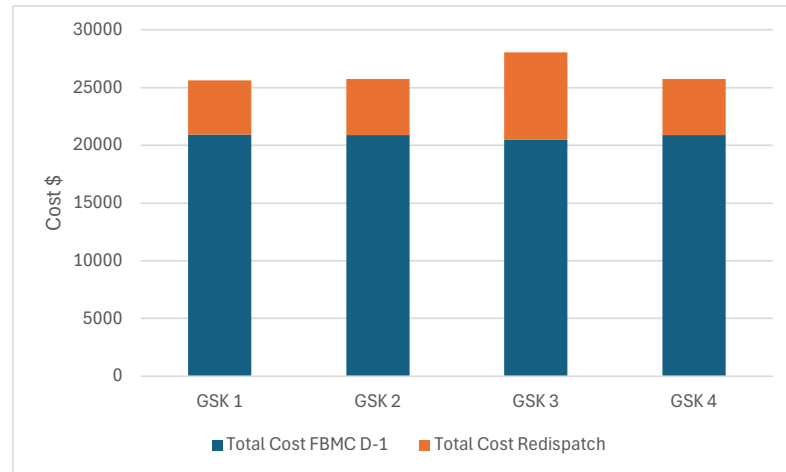


Figure 5.10: The Case 3 Imperfect Forecast

Table 5.8: The Cost Summary Results in Case 4 for Imperfect Forecast

| | GSK 1 | GSK 2 | GSK 3 | GSK 4 |
|--|-----------|-----------|-----------|-----------|
| Total Cost Nodal OPF (\$) | 32805.83 | 32805.83 | 32805.83 | 32805.83 |
| System Marginal Cost Nodal OPF (\$/MWh) | 24.1 | 24.1 | 24.1 | 24.1 |
| Total Cost FBMC D-2 (\$) | 31548.658 | 33356.535 | 34932.306 | 34932.306 |
| System Marginal Cost FBMC D-2 (\$/MWh) | 24.011 | 31.532 | 25.858 | 24.539 |
| Total Cost FBMC D-1 (\$) | 21089.913 | 21004.649 | 20938.949 | 20999.191 |
| System Marginal Cost FBMC D-1 (\$/MWh) | 23.568 | 16.803 | 24.505 | 16.717 |
| Total Cost Redispatch (\$) | 17963.035 | 17248.792 | 17318.846 | 17254.612 |
| System Marginal Cost Redispatch (\$/MWh) | 41.714 | 41.714 | 41.714 | 41.714 |

marginal cost around 16.716 \$/MWh which becomes the lowest marginal cost in the FBMC D-1. An interesting result is shown in the redispatch stage where the GSK 1 has the highest cost compared to the other methods. The GSK 4 also shows a close result to the GSK 2 for the total operational cost.

The result for the total cost of the FBMC and redispatch for the perfect cast can be seen in Figure 5.13. The perfect forecast scenario indicates that slight difference between GSK strategies. The cheapest total cost is obtained by the GSK 2 with \$41796.555. In this scenario, the GSK 4 obtains a similar result with \$42837.169.

In the result for the imperfect scenario as can be seen in Figure 5.14, GSK 1 obtains the highest total cost compared to the others. This result is led by the high redispatch cost. On the other hand, GSK 4 obtained a lower cost compared to GSK 1, with a cost of about \$38253.803. This total cost is close

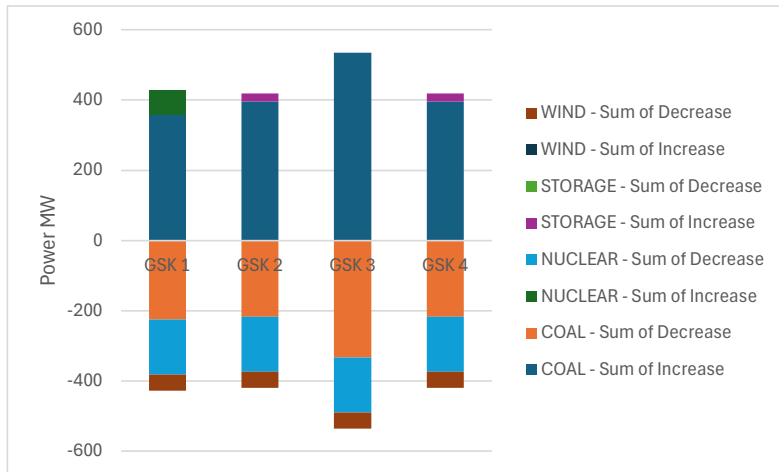


Figure 5.11: The Redispatch Composition for the Case 3 Perfect Forecast

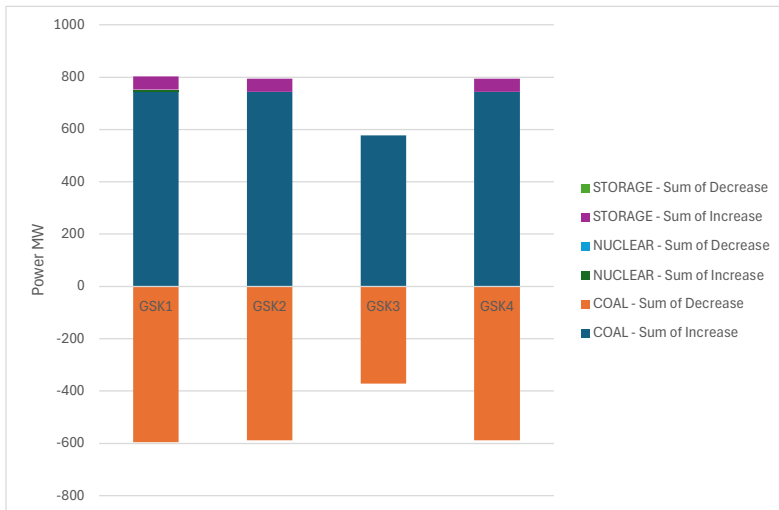


Figure 5.12: The Redispatch Composition Case 3 Imperfect Forecast

to the GSK 2 which obtains a cost around \$38253.441.

In the context of the perfect forecast, the redispatch analysis result for this case is provided in Figure 5.15. The analysis points out that the GSK 4 shows more efficient redispatch power compared to the GSK 1 and 2. This situation is caused by the differences in the composition of each power plant. For instance, in GSK 4, the Natural Gas (NG) power plant is not redispatched to decrease, while it has a large NG decreased output power in GSK 2 with 273.429 MW. These differences between the GSK strategies lead to different redispatch costs.

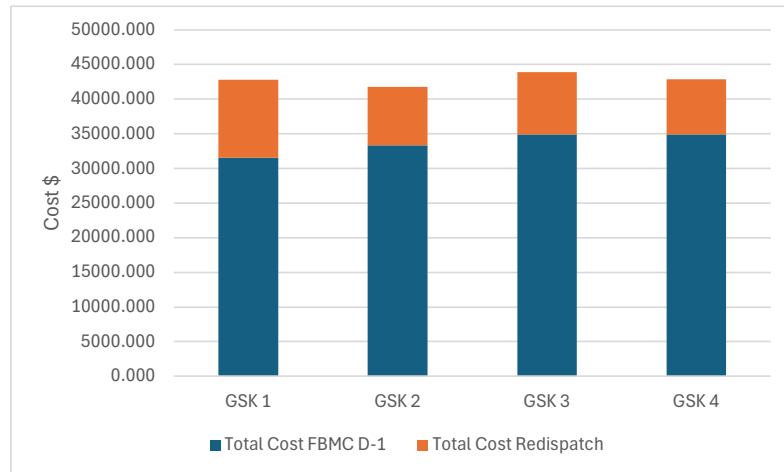


Figure 5.13: The Case 4 Perfect Forecast

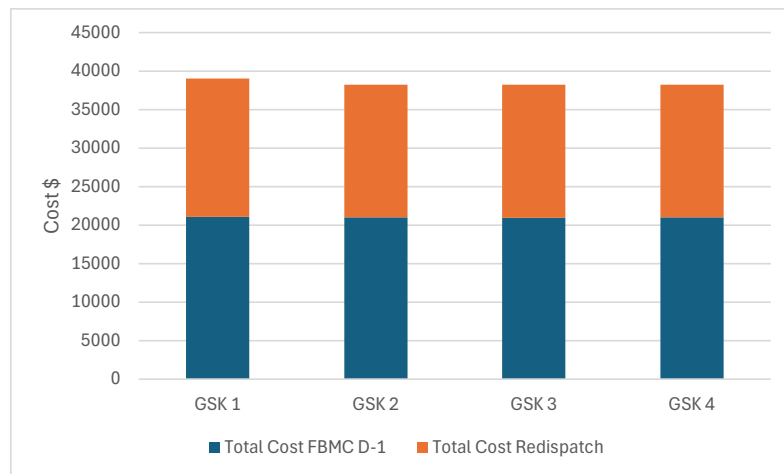


Figure 5.14: The Case 4 Imperfect Forecast

As depicted in Figure 5.16, the redispatch result reflects the effect of forecast inaccuracies. The figure portrays a close result to be redispatched in all of the GSK strategies. Both of these GSKs have a similar combination of power plants. The lowest total power that is needed to redispatch is obtained in the GSK 1. In GSK 1, they prefer to redispatch the Nuclear power plant compared to the others, which choose to redispatch the energy storage.

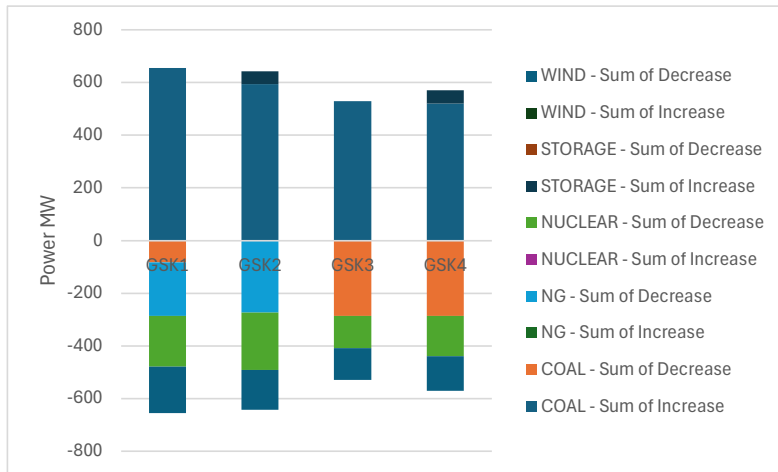


Figure 5.15: The Redispatch Composition for the Case 4 Perfect Forecast

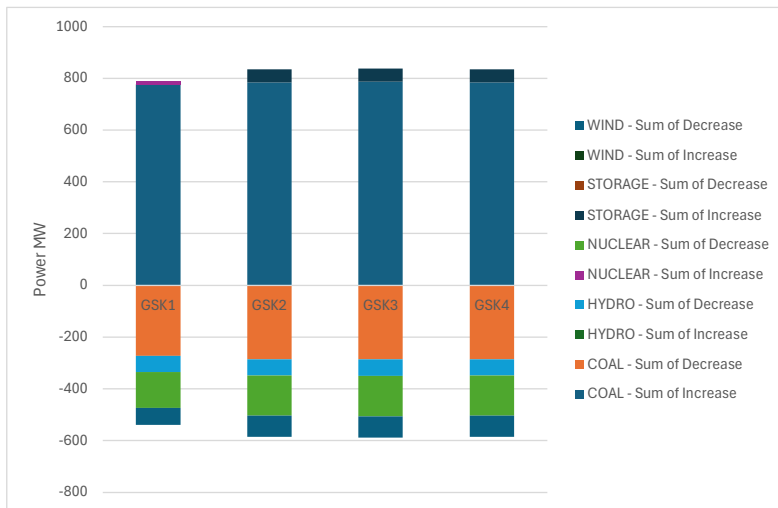


Figure 5.16: The Redispatch Composition Case 4 Imperfect Forecast

5.2 Discussion

Based on the obtained result in the previous section, the proposed GSK strategies have different results related to the case and scenario. In general, the proposed strategy, the GSK 4 has a result close to the GSK 2. The results depicted by the total operational cost, marginal cost, total cost and total redispatch power in the FBMC phase show close performance between these two GSKs. Moreover, the GSK 4 shows an improvement that can be seen through the total operational cost, marginal cost, and redispatch cost in

certain cases and scenarios. For instance, in Case 4, the GSK 4 reduces the total operational cost in the FBMC D-1 compared to the GSK 2 with a cost of around \$ 5.4579. If we assume this margin in one day, it can save up to \$ 130.99. This saving cost is also depicted by the GSK 4 marginal cost in the FBMC D-1, which becomes more efficient with a cost around 16.717 \$/MWh compared to the other GSK. This result shows that GSK 4 more utilizes a lower-cost power plant.

Analyzing the coefficient that exists in the GSK 4, it can be seen that this method represents the GSK 2, which has a more adaptive coefficient in each season. Along the seasons, the GSK 2 has a similar coefficient for each node in the system. This GSK also assigns an equal coefficient to each bus in a zone. However, the GSK 4 can assign a different coefficient in each bus depending on the seasons, considering the total of each zone is always one. This different weight for each bus in the GSK 4 is based on the iteration result that considers the different load and renewable energy resources coefficient in the optimization problem for each season. This GSK also has a feature that can come from the other GSK. For instance, this GSK has a negative attribute that belongs to the GSK 3. Because of this, the GSK also can assign a higher coefficient to the other node which can lead to a lower cost which can be seen in the case 4 for the imperfect scenario.

The adaptability that can be obtained from the proposed GSK strategies offers a solution to the weaknesses of the existing GSK strategies. For instance, GSK 2 assigns all of the nodes based on the average nodes in that zone. This method offers a simple calculation and method, but it does not reflect or consider seasonal situations. This method assigns a similar number of coefficients to the seasons. The other example can come from the GSK 1, which only considers the buses that have a power generation. This method leads to an equal composition to each other of the buses in order to fulfill the total GSK in one zone has to be equal to one.

If the proposed GSK strategy is compared to the GSK 1 and 3, the GSK 4 offers a constant and stable performance. During the cases and scenarios, it can be investigated that the GSK 3 can obtain the lowest position in one season, but it can be the highest spending cost in other seasons. This characteristic is now shown by the proposed GSK.

Based on our discussion and analysis, the proposed GSK strategies can give a new option. This strategy proposed a justified method compared to the existing methods [26] and [27]. This strategy also gives a new opportunity to adapt the system based on the seasons. The proposed GSK strategy also considers the historical data in its optimization and probability in the system

that can lead to a reliable result.

Chapter 6

Conclusions and Future Work

This chapter provides the conclusion of the thesis project and the future work recommendations based on the results and discussion.

6.1 Conclusions

The study of flow-based market coupling (FBMC), as depicted through mathematical formulation and implementation via simulation, has provided insight and understanding into the FBMC process. This research also demonstrates how the FBMC operates when specific cases and scenarios are applied to the system. The exploration of new generation shift keys (GSK) strategies offers additional options and approaches for power system operation and planning, aiming to enhance economic welfare.

To examine the mathematical model that has been discussed, a Python model has been developed to simulate an FBMC process. This Python model provides information related to the planning days in the FBMC process. For each of the planning days, the total cost and system marginal cost are obtained in order to gain the most economical power system operation. The simulation process also includes a forecasting error and different seasons to give a real-world situation to the FBMC process. Through cases and scenarios, the simulation of FBMC successfully depicts real-world conditions.

Based on the obtained result and analysis, the proposed GSK strategy demonstrates flexibility and adaptability over traditional GSK approaches. The proposed strategy shows seasonal sensitivity and assigns varying weights across buses while maintaining zonal balance, enhancing its responsiveness to load and renewable energy variations. The strategy offers an adaptive framework that reflects seasonal patterns and system uncertainties more

realistically than the static and uniform coefficients used in the existing GSK strategies.

The results also show that the proposed GSK strategies obtain efficiency in the total cost and system marginal cost in the FBMC optimization processes. The proposed GSK strategy reduces the total cost of operation around \$ 5.4579 in a case, and it can save up to \$ 130.99 in one day by assuming a similar margin in one day.

This new GSK strategy gives new options to the planner and operator in order to obtain the most reliable and economical approach in power system operation related to the FBMC. The proposed GSK strategy can be used interchangeably during the year and substitute the existing GSK strategies because of their cost efficiency. These new options can lead to an increase in economic welfare in power system operations in the future.

6.2 Future work

Due to the complexity of modeling the power system components and limitations in research data, there are missing parameters and considerations as follows

6.2.1 The Power Plant Model and Parameters

The power plant modeling in this research is limited by the availability of data. To enhance the reliability of the optimization, parameters such as ramp-up and ramp-down rates, start-up and shut-down times, as well as minimum up and down times, can be included. Incorporating these parameters would result in a model that more closely reflects real-world conditions and yields more realistic optimization results.

6.2.2 Running Period Test

To obtain a broader perspective on the FBMC simulation and GSK results, a long-term simulation period can be implemented. This extended period could span 24 hours, one week, one month, or even an entire year.

6.2.3 Data Scope and Scale

The data used in this research is limited to a test case study. To gain a deeper understanding and insights into the impact of FBMC simulation and GSK

strategies, the approach can be extended to a larger-scale system, such as a country, region, or continent.

6.3 Reflections

Reflecting on the initial goal of flow-based market coupling, continuous development and improvement must be carried out to obtain more reliable results in power system operation. These improvements are necessary to address and manage the large-scale integration of renewable energy resources in the future. This work on FBMC can contribute to the United Nations (UN) Sustainable Development Goals (SDGs) 7, 8, 9, and 13 in support of a more sustainable living planet.

References

- [1] K. Van Den Bergh, J. Boury, and E. Delarue, “The Flow-Based Market Coupling in Central Western Europe: Concepts and definitions,” en, *The Electricity Journal*, vol. 29, no. 1, pp. 24–29, Jan. 2016, ISSN: 10406190. DOI: [10.1016/j.tej.2015.12.004](https://doi.org/10.1016/j.tej.2015.12.004). Accessed: May 9, 2025. [Online]. Available: <https://linkinghub.elsevier.com/retrieve/pii/S104061901530004X>.
- [2] *Flow-Based in the Nordics – Is the Media Uproar Fair?* sv. Accessed: May 9, 2025. [Online]. Available: <https://www.flower.se/insights/knowledge/flow-based-in-the-nordics-is-the-media-uproar-fair/>.
- [3] E. B. Brose, A. S. Haugsbø, E. Bjørndal, and M. H. Bjørndal, “Flow-Based Market Coupling in the Nordic Power Market,” en,
- [4] A. H. Bo, V. Viken Kallset, I. Oleinikova, H. Farahmand, and K. L. Refsnas, “The impact of Flow-Based Market Coupling on the Nordic region,” en, in *2020 17th International Conference on the European Energy Market (EEM)*, Stockholm, Sweden: IEEE, Sep. 2020, pp. 1–6, ISBN: 978-1-7281-6919-4. DOI: [10.1109/EEM49802.2020.9221952](https://doi.org/10.1109/EEM49802.2020.9221952). Accessed: May 9, 2025. [Online]. Available: <https://ieeexplore.ieee.org/document/9221952/>.
- [5] *Successful go-live of the Nordic Flow-based Market Coupling project*, en, Nov. 2024. Accessed: May 9, 2025. [Online]. Available: <https://www.svk.se/en/about-us/news/news/successful-go-live-of-the-nordic-flow-based-market-coupling-project/>.
- [6] E. Bjørndal, M. Bjørndal, and H. Cai, “Flow-Based Market Coupling in the European Electricity Market – A Comparison of Efficiency and Feasibility,” Oct. 2018, ISSN: ISSN: 1500-4066. DOI: <https://dx.doi.org/10.2139/ssrn.3272188>.

- [7] S. Voswinkel, B. Felten, T. Felling, and C. Weber, *What Drives Welfare in Europe's Approach to Electricity Market Coupling?* en, SSRN Scholarly Paper, Rochester, NY, Jul. 2019. doi: [10.2139/ssrn.3424708](https://doi.org/10.2139/ssrn.3424708). Accessed: Mar. 7, 2025. [Online]. Available: <https://papers.ssrn.com/abstract=3424708>.
- [8] B. Felten, T. Felling, P. Osinski, and C. Weber, "Flow-Based Market Coupling Revised - Part I: Analyses of Small- and Large-Scale Systems," en, *SSRN Electronic Journal*, 2019, ISSN: 1556-5068. doi: [10.2139/ssrn.3404044](https://doi.org/10.2139/ssrn.3404044). Accessed: May 31, 2025. [Online]. Available: <https://www.ssrn.com/abstract=3404044>.
- [9] C. Byers and G. Hug, "Modeling flow-based market coupling: Base case, redispatch, and unit commitment matter," in *2020 17th International Conference on the European Energy Market (EEM)*, ISSN: 2165-4093, Sep. 2020, pp. 1–6. doi: [10.1109/EEM49802.2020.9221922](https://doi.org/10.1109/EEM49802.2020.9221922). Accessed: Feb. 27, 2025. [Online]. Available: <https://ieeexplore.ieee.org/document/9221922>.
- [10] *ENTSO-E Transparency Platform*. Accessed: Jun. 3, 2025. [Online]. Available: <https://transparency.entsoe.eu/>.
- [11] Svenska kraftnät, *Statistics*, en, Mar. 2021. Accessed: Jun. 3, 2025. [Online]. Available: <https://www.svk.se/en/stakeholders-portal/electricity-market/statistics/>.
- [12] ENTSO-E, *Single Day-ahead Coupling (SDAC)*, English. [Online]. Available: https://www.entsoe.eu/network_codes/cacm/implementation/sdac/.
- [13] *European Market Coupling*.
- [14] *Price Coupling of Regions (PCR)*. Accessed: Jun. 2, 2025. [Online]. Available: <https://www.nordpoolgroup.com/en/the-power-market/Day-ahead-market/Price-coupling-of-regions/>.
- [15] Synertics, *Understanding Market Coupling*, en. Accessed: Jun. 2, 2025. [Online]. Available: <https://synertics.io/blog/68/understanding-market-coupling>.
- [16] *What is market coupling and how is the European electricity market interlinked? We explain: Definition, history, cross boarder trading (XBID), FBMC and more*, en-US. Accessed: Jun. 2, 2025. [Online]. Available: <https://www.next-kraftwerke.com/knowledge/market-coupling>.

- [17] *Market coupling*, Nov. 2013. [Online]. Available: <https://www.emissions-euets.com/internal-electricity-market-glossary/481-market-coupling>.
- [18] K. Fehér, “INSIGHTS TO THE DAY AHEAD MARKET COUPLING PROJECTS,” en,
- [19] *Mission Statement*, en-us. Accessed: May 9, 2025. [Online]. Available: <https://www.entsoe.eu/about/inside-entsoe/objectives/>.
- [20] Nordic RCC, *The Nordic Capacity Calculation methodology (CCM) project stakeholder Forum*. [Online]. Available: https://nordic-rcc.net/wp-content/uploads/2019/12/20191212-Nordic-CCM-SHF_V0.pdf.
- [21] *Simulation Results*, en-US. Accessed: Jun. 4, 2025. [Online]. Available: <https://nordic-rcc.net/flow-based/simulation-results/>.
- [22] epexspot, *Go-live of Nordic flow-based CCM delayed to Q1 2024 | EPEX SPOT*. Accessed: Jun. 4, 2025. [Online]. Available: <https://www.epexspot.com/en/news/go-live-nordic-flow-based-ccm-delayed-q1-2024>.
- [23] B. E. Bjerrum, *Nordic Flow-Based Market Coupling Project confirms Go-Live for 29th October 2024*, en-US, Oct. 2024. Accessed: Jun. 4, 2025. [Online]. Available: <https://nordic-rcc.net/nordic-flow-based-market-coupling-project-confirms-go-live-for-29th-october-2024/>.
- [24] D. Biggar and M. R. Hesamzadeh, *The economics of electricity markets* (Wiley - IEEE), en. Chichester, West Sussex, United Kingdom: Wiley, 2014, ISBN: 978-1-118-77575-2 978-1-118-77574-5 978-1-118-77572-1 978-1-118-77573-8. DOI: 10.1002/9781118775745.
- [25] M. Amelin and L. Söder, *Efficient Operation and Planning of Power Systems - 2011*, English. [Online]. Available: <https://kth.diva-portal.org/smash/record.jsf?pid=diva2%3A467471>.

- [26] R. Weinhold and R. Mieth, “Uncertainty-Aware Capacity Allocation in Flow-Based Market Coupling,” en, *IEEE Transactions on Power Systems*, vol. 39, no. 1, pp. 147–159, Jan. 2024, ISSN: 0885-8950, 1558-0679. doi: 10.1109/TPWRS.2023.3265320. Accessed: May 8, 2025. [Online]. Available: <https://ieeexplore.ieee.org/document/10094020/>.
- [27] C. Dierstein, “Impact of Generation Shift Key determination on flow based market coupling,” in *2017 14th International Conference on the European Energy Market (EEM)*, ISSN: 2165-4093, Jun. 2017, pp. 1–7. doi: 10.1109/EEM.2017.7981901. Accessed: Feb. 27, 2025. [Online]. Available: <https://ieeexplore.ieee.org/document/7981901/?arnumber=7981901>.
- [28] ENTSO-E, *ENTSO-E generation AND LOAD SHIFT KEY implementation GUIDE*. [Online]. Available: https://eepublicdownloads.entsoe.eu/clean-documents/EDI/Library/lisig/161027_MC_TOP_9a_Generation_and_Load_Shift_Key_Implementation_Guide_v2.pdf.
- [29] *Establishing a guideline on capacity allocation and congestion management*, English, Jul. 2015. [Online]. Available: https://www.acer.europa.eu/sites/default/files/documents/Recommendations_annex/ACER%20Recommendation%2002-2021%20on%20CACM%20-%20Annex%201%20-%20CACM%20Regulation.pdf#:~:text=%E2%80%99generation%20shift%20key%E2%80%99%20means%20a,in%20the%20common%20grid%20model.
- [30] A. Marien, P. Luickx, A. Tirez, and D. Woitrin, “Importance of design parameters on flowbased market coupling implementation,” in *2013 10th International Conference on the European Energy Market (EEM)*, ISSN: 2165-4093, May 2013, pp. 1–8. doi: 10.1109/EEM.2013.6607298. Accessed: May 31, 2025. [Online]. Available: <https://ieeexplore.ieee.org/document/6607298/>.
- [31] *Supporting document for the Nordic capacity Calculation Region’s proposal for capacity calculation methodology in accordance with Article 20(2) of commission Regulation (EU) 2015/1222 of 24 July 2015 establishing a guideline on capacity allocation and congestion management*, English. [Online]. Available: <https://nordic-rcc.net/wp-content/uploads/2018/10/Stakeholder-consultation-document-and-Impact-Assessment-for->

the-Capacity-Calculation-Methodology-Proposal-for-the-Nordic-CCR.pdf#:~:text=The%20FB%20approach%20makes%20use,might%20result%20in%20a%20large.

- [32] B. Jegleim, “Flow Based Market Coupling,” en,
- [33] T. Kristiansen, “The flow based market coupling arrangement in Europe: Implications for traders,” *Energy Strategy Reviews*, vol. 27, p. 100444, Jan. 2020, ISSN: 2211-467X. DOI: 10.1016/j.esr.2019.100444. Accessed: May 31, 2025. [Online]. Available: <https://www.sciencedirect.com/science/article/pii/S2211467X19301373>.
- [34] C. Hagedorn, “CWE Flow Factor Competition, part II: Quantitative Analysis,” en,
- [35] J. G. Møller, *Overview of settings at flow-based go-live*. [Online]. Available: <https://nordic-rcc.net/wp-content/uploads/2024/09/05-Overview-of-settings-at-flow-based-go-live.pdf>.
- [36] M. L. Bynum et al., *Pyomo — Optimization Modeling in Python* (Springer Optimization and Its Applications), en. Cham: Springer International Publishing, 2021, vol. 67, ISBN: 978-3-030-68927-8 978-3-030-68928-5. DOI: 10.1007/978-3-030-68928-5. Accessed: May 31, 2025. [Online]. Available: <http://link.springer.com/10.1007/978-3-030-68928-5>.
- [37] *GLPK - GNU Project - Free Software Foundation (FSF)*. Accessed: May 31, 2025. [Online]. Available: <https://www.gnu.org/software/glpk/#introduction>.
- [38] T. Felling, B. Felten, P. Osinski, and C. Weber, *Flow-Based Market Coupling Revised - Part II: Assessing Improved Price Zones in Central Western Europe*, en, SSRN Scholarly Paper, Rochester, NY, Jun. 2019. DOI: 10.2139/ssrn.3404046. Accessed: May 31, 2025. [Online]. Available: <https://papers.ssrn.com/abstract=3404046>.
- [39] NREL, *GridMod/RTS-GMLC*, original-date: 2017-01-13T22:10:37Z, May 2025. Accessed: Jun. 1, 2025. [Online]. Available: <https://github.com/GridMod/RTS-GMLC>.

- [40] *Normalization (statistics)*, en, Page Version ID: 1292226400, May 2025. Accessed: Jun. 4, 2025. [Online]. Available: [https://en.wikipedia.org/w/index.php?title=Normalization_\(statistics\)&oldid=1292226400](https://en.wikipedia.org/w/index.php?title=Normalization_(statistics)&oldid=1292226400).
- [41] ACER, *Day-ahead capacity calculation methodology of the Core capacity calculation region*. [Online]. Available: <https://eepublicdownloads.entsoe.eu/clean-documents/nc-tasks/ACER%20Decision%2002-2019%20on%20CORE%20CCM-combined.pdf>.

TRITA-EECS-EX-2025:937
Stockholm, Sverige 2024

www.kth.se